

School of Science

**The Effect of Ionic Liquids Solvents on the
Dehydration of Alcohols**

Bhavana Kapila

A thesis submitted to attain the
requirements for the degree of

Masters of Philosophy

Auckland University of Technology

March 2020

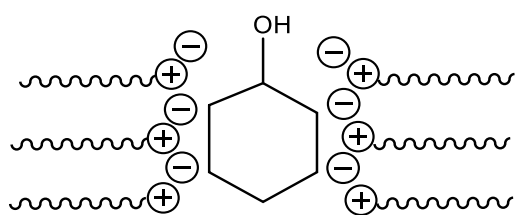
Abstract

Ionic liquids have a unique combination of intermolecular interactions that give rise to unusual structure features including the formation of amphiphilic nanostructures with well-defined polar and non-polar domains. The effect of these nanostructures remains poorly understood. The aim of this thesis was to examine these effects of the structure of ionic liquid solvents using the dehydration of alcohols as a model reaction. Several ionic liquids containing 1-alkyl-3-methylimidazolium cations and different anions were synthesized to explore these effects. Secondary alcohols cyclohexanol and octan-2-ol were found to undergo dehydration reactions in these imidazolium ionic liquids at elevated temperatures in hydrothermal reactors. Alkenes were formed as the major product, with traces of the corresponding ketones and ethers.

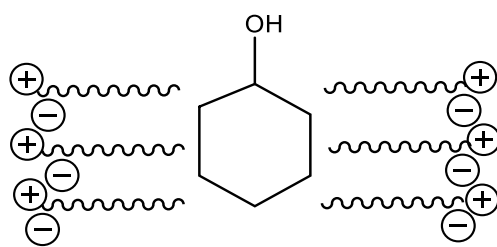
The ionic liquid anion influenced the reactivity of these alcohol dehydration reactions. Hydrophobic, weakly interacting anions such as $[\text{NTf}_2]^-$ lead to more effective dehydration reactions compared to more strongly interacting, hydrophilic anions such as $[\text{OTf}]^-$ and $[\text{Me}_2\text{PO}_4]^-$ which gave trace or no products with alcohols. Increasing the mole fraction of reactants was found to decrease the formation of products, the opposite to the trend that would be expected for an innocent solvent which highlights that the ionic liquid plays an active role in the reactivity.

Increasing the alkyl chain length of the cation had anion-dependent effects on reactivity. This increased the reactivity of the alcohol when the $[\text{OTf}]^-$ anion was used while decreasing reactivity for imidazolium ionic liquids with the $[\text{NTf}_2]^-$ anion.

The catalytic activity of ionic liquids reveals the structural and nanostructural effects of ionic liquids in alcohol dehydration reactions. The amphiphilic nanostructure contains a polar domain consisting of the catalytically active ionic network and inactive apolar alkyl chain domain. Hence the $[\text{OTf}]^-$ anion increases the proportion of alcohol in the polar domain with its effective concentration increased for long imidazolium ionic liquid alkyl chain lengths. The $[\text{NTf}_2]^-$ anion does not encourage the same partitioning into the polar region and the exclusion of the alcohol increases with increased alkyl chain length, accounting for the change in the reactivity trend. These results indicate that the amphiphilic nanostructure of ionic liquids can influence the outcome of alcohol dehydration reactions.



Fast Reaction



Slow Reaction

Acknowledgement

I spent almost five months in AUT as MPhil student from March 2019 to July 2019 was important time as I developed my prospective. After which I shifted to University of Auckland to complete my rest of the lab work with my supervisor. In my life I had many experiences and good time that I think will impact me professionally throughout my progress.

Most prominently, I would like to acknowledge full heartedly my supervisor, Dr. Cameron Weber, University of Auckland, who's heartening, keeping up always, direction from the initial to the final end help me in evolving the comprehension of the project. I am relieved for his inducement, individuality and management during whole of my project from his buzzing schedule. He was always in mind set to work out on the strenuous situations to understand and resolve them. He helped me to understand the obscure concepts during project with his all possible efforts during project when required. When he shifted to University of Auckland by his attempts, he made space available for me in lab and office place there, that helped me to continue my project conveniently in his supervision. Thank you for being always encouraging and for contributing many hours on the thesis.

I also want to thank Allan Blackman who motivated me to take the right decision about my choice of course when I came AUT. Whenever, I went to him with my any problem regarding the lab and my project he solved it for me.

I express my great thanks to Navneet Brar, one of the group members, helped me to understand the calculations and concepts. I always discussed my work with her and she hear me, tried to correct me in carrying out my experiments. I asked her about my uncertainties in experiments and got instant replies from her despite busy with her own work. I also like thank Henry, Emma for the ILs and to Navjot and Stefy for helping me during my thesis.

I am also thankful to the technicians Iana Gritcan, Adrian Owens and Tony Chen who made the lab keep on going smoothly, for running my samples on GC-MS and help in solving problems related to the syringe on GC-FID. I also thankful to Radesh Singh (Lab Technician) and Dr. Michael Schnitz for maintaining the NMR facilities in University of Auckland.

I would also like to express my huge thanks to my in-laws who finance my studies. I'm thankful to my own parents who are still concerned for me, as I am not with them due to my studies when they really need me. Last but not the least I am thankful to my husband for his moral support during my thesis writing.

The cheerful memories created during a year that I experienced to work in both the universities.
Thank you everyone.

Abbreviations

ACN	acetonitrile
AILs	aprotic ionic liquids
[C _n C ₁ im]	1-alkyl-3-methylimidazolium
[C _n py]	1-alkylpyridinium
[C _n C ₁ pyrr]	1-alkyl-3-methylpyrrolidinium
[C _n C ₁ im] ⁺	1-alkyl-3-methylimidazolium cation
DBSA	dodecylbenzenesulfonic acid
DMSO-d ₆	deuterated dimethyl sulfoxide
DMSO	dimethylsulfoxide
°C	degrees Celsius
E ₁	unimolecular elimination reaction
E ₂	bimolecular elimination reaction
equiv.	equivalent
GC-MS	gas chromatography- mass spectroscopy
GC-FID	Gas Chromatography- Flame Ionization Detector
g	gram
H-bonding	hydrogen-bonding
IR	infrared
ILs	ionic liquids
ICP-MS	Inductively Coupled Plasma Mass Spectrometry
m.p.	melting point
4-MBA	4-methoxybenzyl alcohol
mL	milliliter

MS-CG	Multiscale Coarse-Graining
MHz	mega hertz
min ⁻¹	per minute
mol	mole
μL	microlitre
NMR	Nuclear Magnetic Resonance
[NTf ₂] ⁻	bis(trifluoromethylsulfonyl)imide
(n-BuOs-Bu)	[3,3,-dimethylpropyl]methyl ether
[OTf]	trifluoromethanesulfonate
PILs	protic ionic liquids
ppm	parts per million
[P _{666,14}][DBS]	triethyl-tetradecylphosphonium dodecylbenzene sulfonate
NaOTf	sodium triflate
TsOH	p-toluene sulfonic acid
TMP	trimethyl phosphate
wt %	weight percent

Table of Contents

Abstract.....	i
Acknowledgement.....	iii
Abbreviations.....	v
Attestation of Authorship.....	x
List of Figures.....	xi
List of Tables.....	xiii
List of Schemes.....	xiv
CHAPTER 1: INTRODUCTION.....	1
1.1. Ionic liquids	2
1.2. Classification of Ionic Liquids	4
1.3. Structure of Ionic Liquids	4
1.3.1. Hydrogen bonding	5
1.3.2. Amphiphilic Nanostructure	7
1.4. Alcohol Dehydration Mechanism	9
1.5. Alcohol Dehydration In Ionic Liquids	11
1.6. Project Aim.....	13
CHAPTER 2: EXPERIMENTAL	14
2.1. General.....	15
2.2. Physical Measurements	15
2.2.1. NMR.....	15
2.2.2. Gas Chromatography with Flame Ionization Detector (GC-FID).....	15
2.2.3. Method for GC-FID Analysis	15
2.2.4. Method for GC-MS Analysis	16
2.2.5. Analysis by ICP-MS.....	16
2.3. General Procedures	16
2.3.1. Dehydration of alcohols.....	16
2.3.1.1 Extraction of products by using column chromatography	16
2.3.1.2 Extraction of products using solvent extraction.....	17
2.3.2. GC-FID Calibration.....	17
2.4. Synthesis of Ionic Liquids	17
2.4.1. Synthesis of 1-decyl-3-methylimidazolium chloride [C₁₀C₁im]Cl.....	17
2.4.2. Synthesis of 1-decyl-3-methylimidazolium bis(trifluoromethane- sulfonyl)imide [C₁₀C₁im][NTf₂]	18
2.4.3. Synthesis of 1-decyl-3-methylimidazolium bis(trifluoromethane- sulfonyl)imide [C₁₀C₁im][NTf₂]	19

2.4.4. Synthesis of 1-decyl-3-methylimidazolium trifluoromethanesulfonate	20
[C ₁₀ C ₁ im][OTf]	20
2.4.5. Synthesis of 1-decyl-3-methylimidazolium dimethylphosphate	20
[C ₁₀ C ₁ im][Me ₂ PO ₄]	20
2.4.6. Synthesis of 1-octyl-3-methylimidazolium chloride [C ₈ C ₁ im]Cl	21
2.4.7. Synthesis of 1-hexyl-3-methylimidazolium chloride [C ₆ C ₁ im]Cl	22
2.4.8. Synthesis of 1-octyl-3-methylimidazolium bis(trifluoromethyl- sulfonyl)imide [C ₈ C ₁ im][NTf ₂].....	23
2.4.9. Synthesis of 1-hexyl-3-methylimidazolium bis(trifluoromethyl- sulfonyl)imide [C ₆ C ₁ im][NTf ₂].....	23
2.4.10. Synthesis of 1-octyl-3-methylimidazolium trifluoromethanesulfonate	24
[C ₈ C ₁ im][OTf]	24
2.4.11. Synthesis of 1-hexyl-3-methylimidazoliumtrifluoromethanesulfonate	25
[C ₆ C ₁ im][OTf]	25
CHAPTER 3: RESULTS AND DISCUSSINS	26
3.1. Synthesis of Ionic Liquids	27
3.1.1. Synthesis of Imidazolium Halides Ionic Liquids.....	27
3.1.2. Synthesis of Imidazolium Dimethyl phosphate Ionic Liquids	28
3.1.3. Synthesis of Imidazolium Trifluoromethanesulfonate Ionic Liquids	28
3.1.4. Synthesis of Imidazolium bis(trifluoromethylsulfonyl)imide ILs	29
3.2. Set up of Model Reactions	29
3.2.1. Dehydration of Alcohol as a Model Reaction	29
3.2.2. Tert. Amyl Alcohol and Methanol.....	30
3.2.3. 1,4-Cyclohexandiol.....	31
3.2.4. Octan-1-ol	31
3.2.5. Octan-2-ol	32
3.2.6. Cyclohexanol	35
3.3. Analytical Protocol.....	37
3.3.1. Selection of Internal Standard.....	37
3.4. Establishing the GC-FID Method analysis	40
3.4.1. Cyclohexanol Calibration.....	40
3.4.2. Cyclohexanol Calibration 2.....	43
3.4.3. Octan-2-ol GC-FID Method.....	44
3.4.3.1 Octan-2-ol Calibration.....	46
3.5. Development of an extraction method for the quantification of.....	48
products	48
3.5.1. Silica Chromatography Column Extraction	49

3.6. Extraction methods with quantification of products on GC-FID	49
3.7. Cyclohexanol Reactivity with Different Ionic Liquids	53
3.8. Effect of Cyclohexanol Mole Fraction on Reactivity	54
3.9. Effect of Ionic Liquid Anion on Cyclohexanol Dehydration	56
3.10. Mechanism of Cyclohexanol Dehydration in Ionic Liquids.....	57
3.11. Reactivity of Octan-2-ol within Ionic Liquids	59
CHAPTER 4: CONCLUSIONS & FUTURE WORK	61
4.1. Conclusions	62
4.2. Future Work.....	63
References.....	64

Attestation of Authorship

I hereby declare that this submission is my own work and that, to the best of my knowledge and belief, it contains no material previously published or written by another person (except where explicitly defined in the acknowledgements), nor material which to a substantial extent has been submitted for the award of any other degree or diploma of a university or other institution of higher learning.

List of Figures

Figure 1. Cations in Ionic liquids (Adapted from Ref. 6).....	2
Figure 2. Common anions for Ionic liquids (Adapted from Ref. 6).....	3
Figure 3. Structural Arrangement of ions in Protic and Aprotic ILs (Adapted from Ref.17)...	4
Figure 4. Arrangement of cations and anions in molten salts and ionic liquids. (Adapted from reference17).	5
Figure 5. Position of H atoms on imidazolium ring (Adapted from Ref. 26).....	6
Figure 6. Imidazolium cation showing association sites for anion (Adapted from ref. 27).....	7
Figure 7. Structure of stimulation for ion pairs. (a) all atoms, (b)tail groups, (c)head groups only, and (d)anions only (Adapted from ref .30).....	8
Figure 8. X-ray diffraction pattern from the series of RTILs: [C _n C ₁ im]Cl n=3,4,6,8,10 at 25°C.L= spatial correlation, n= the alkyl chain length.(Adapted from Ref. 31).	8
Figure 9. Bulk structure of [C _n C ₁ mim] [PF ₆] with n=2-12 (Adapted from Ref. 13).....	9
Figure 10. ¹ H NMR after 120 hours for the reaction of octan-1-ol in [C ₁₀ C ₁ im][NTf ₂].	32
Figure 11. ¹ H NMR after 24hours for reaction of octan-2-ol in [C ₁₀ C ₁ im][NTf ₂]at 180°C. ...	35
Figure 12. ¹ HNMR showing the formation of cyclohexene from cyclohexanol after two hours at 180°C in [C ₁₀ C ₁ im] [NTf ₂].....	37
Figure 13. ¹ HNMR before reaction of octan-2-ol and [C ₁₀ C ₁ im][NTf ₂] exploring the stability of mesitylene as an internal standard.	38
Figure 14. ¹ HNMR after 24hours of reaction between octan-2-ol and [C ₁₀ C ₁ im][NTf ₂] with mesitylene as an internal standard.	39
Figure 15. GC-FID chromatogram of a cyclohexanol reaction mixture with major products assigned.....	40
Figure 16. GC-FID chromatogram of cyclohexanol standards.....	41
Figure 17. GC-FID calibration curve for cyclohexanol.....	42
Figure 18. GC-FID calibration curve for cyclohexene.	42
Figure 19. GC-FID calibration curve for cyclohexanone.	43
Figure 20. Cyclohexanol GC-FID calibration curve.....	43
Figure 21. Cyclohexene GC-FID calibration curve.....	44

Figure 22. Cyclohexanone GC-FID calibration curve.....	44
Figure 23. Products of octan-2-ol separation on GC-FID.....	45
Figure 24. Octan-2-ol standards separation on GC-FID.....	46
Figure 25. GC-FID Calibration curve of octan-2-ol.....	47
Figure 26. GC-FID Calibration curve of oct-1-ene.....	47
Figure 27. GC-FID Calibration curve of trans-2-octene.....	48
Figure 28. GC-FID Calibration curve of octan-2-one.....	48
Figure 29. Cyclohexanol conversion and cyclohexene yield at different mole fraction of cyclohexanol in [C ₁₀ C ₁ im] [NTf ₂].	55
Figure 30. ³¹ P NMR of reaction 23 after reaction.....	57

List of Tables

Table 1. Results from ¹ HNMR spectroscopy with mesitylene or acetophenone as standard Adapted from Ref 38.....	12
Table 2. Results of reactions between tert-amyl alcohol and methanol in [C ₁₀ C _{1im}][NTf ₂]. Reactants and IL were prepared in a volume ratio of tert-amyl alcohol: methanol: IL of 1:2:3.	31
Table 3. Results of initial reactions of octan-2-ol in [C ₁₀ C _{1im}][NTf ₂]	33
Table 4. Relative Integrals of alkene peak at 5.4 versus octan-2-ol peak at 3.8	34
Table 5. Cyclohexanol dehydration in [C ₁₀ C _{1im}][NTf ₂] under different reaction conditions.....	366
Table 6. Dehydration reaction to check the reactivity of mesitylene with octan-2-ol in presence of [C ₁₀ C _{1im}][NTf ₂]	38
Table 7. Mass ratio of cyclohexanol calibration standards used for GC-FID analysis.....	41
Table 8. Silica column separation of reactions 6 and 8 using dichloromethane as an eluent .	49
Table 9. Dehydration of cyclohexanol in [C ₁₀ C _{1im}][NTf ₂] using mesitylene as an internal standard with the quantification of products by GC-FID after separation using a silica. Reported errors are standard deviations of replicate experiments where replicates were performed.....	50
Table 10. Dehydration of cyclohexanol in [C ₁₀ C _{1im}][NTf ₂] using mesitylene as an internal standard with the quantification of products by GC-FID after hexane extraction. Reported errors are standard deviations of replicate experiments.....	51
Table 11. Cyclohexanol dehydration reaction with [C ₁₀ C _{1im}] [NTf ₂] and IS at changed reaction conditions.....	52
Table 12. Cyclohexanol reactivity with different [C _n C _{1im}][NTf ₂] ILs at 180°C for 3hours analysed by GC-FID. Reported errors are standard deviations of replicate experiments.....	53
Table 13. Quantification of products on GC-FID after cyclohexanol reactivity with two [OTf] (reaction 25, 26), [C ₁₀ C _{1im}] [Me ₂ PO ₄] and, [C ₄ C _{1im}] [N(CN) ₂] (reaction 29, 30) ILs at 180°C for 3 hours and with same temperature and same OTf ILs for 18 hours (reaction 27, 28)	56
Table 14. Quantification of products on GC-FID after octan-2-ol reactivity with ILs containing [NTf ₂] ⁻ and [OTf] ⁻ anion with different alkyl chains at 180°C for 3 hours. Table 14. Quantification of products on GC-FID after octan-2-ol reactivity with ILs containing [NTf ₂] ⁻ and [OTf] ⁻ anion with different alkyl chains at 180°C for 3 hours.	59

List of Schemes

Scheme 1. E ₁ Reaction (Adapted from Ref. 35).....	10
Scheme 2. E ₂ reaction mechanism.....	10
Scheme 3. 4-methoxybenzyl alcohol etherification dehydration in [P666,14][DBS] and [C ₄ C ₁ im][PF ₆] (Adapted from Ref.38).....	12
Scheme 4. Synthesis of [C ₁₀ C ₁ im][Cl]	17
Scheme 5. Synthesis of [C ₁₀ C ₁ im][NTf ₂]	18
Scheme 6. Synthesis of [C ₁₀ C ₁ im][NTf ₂]	19
Scheme 7. Synthesis of [C ₁₀ C ₁ im][OTf]	20
Scheme 8. Synthesis of [C ₁₀ C ₁ im][Me ₂ PO ₄]	20
Scheme 9. Synthesis of [C ₈ C ₁ im]Cl	21
Scheme 10. Synthesis of [C ₆ C ₁ im]Cl	22
Scheme 11. Synthesis of [C ₈ C ₁ im][NTf ₂]	23
Scheme 12. Synthesis of [C ₆ C ₁ im][NTf ₂]	23
Scheme 13. Synthesis of [C ₈ C ₁ im][OTf].....	24
Scheme 14. Synthesis of [C ₆ C ₁ im][OTf].....	25
Scheme 15. General mechanism for the formation of 1-alkyl-3-methylimidazolium chlorides.	27
Scheme 16. General mechanism for the formation of 1-alkyl-3-methylimidazolium dimethylphosphate.	28
Scheme 17. General reaction for the formation of Tert. Amyl methyl ether.....	30
Scheme 18. General reaction for dehydration of Octan-2-ol.....	33
Scheme 19. Proposed mechanism for the dehydration of cyclohexanol in ILs.....	58

CHAPTER 1: INTRODUCTION

1.1. Ionic liquids

Liquids are the states of matter intermediate between solids and gases. Ionic liquids are liquids comprised of ions which melt below 100°C. In 1914, ethyl ammonium nitrate (m.p 12°C), was identified by Paul Walden, and was the first example of a salt in its liquid form at room temperature.¹ In 1951, Hurley and Weir discovered the room temperature liquid 1-ethylpyridinium bromide-aluminium chloride.² In 1992, air and moisture stable 1-ethyl-3-methylimidazolium ILs were developed by Wilkes and Zaworotko.³ The discovery of the bis(trifluoromethylsulfonyl)imide anion [NTf₂]⁻ by Bonhote et al. in 1996 increased the variety of cations that could be used to prepare ILs, due to the weakly interacting, charge delocalized nature of this anion.⁴

ILs characteristically display properties including low vapor pressures and electrical conductivity. They are often non-flammable and recyclable. ILs have been utilized in applications for catalysts, material synthesis, liquid crystals, separation processes as well as in electrochemistry. Some common cations and anions used in ILs are shown in Figures 1 and 2.⁵

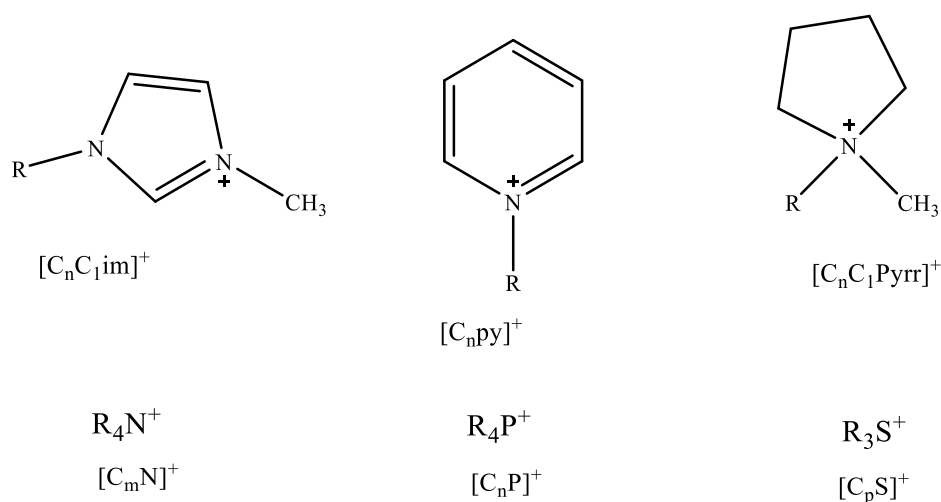


Figure 1. Cations in ionic liquids (Adapted from Ref⁶).

The low vapor pressures of ILs are due to the strong ionic interactions present. Unlike organic solvents they don't suffer from evaporation losses, leading to interest in the use of ILs as recyclable solvents. ILs do not contribute air pollution due to these low vapor pressures.

Despite not contributing directly to air pollution ILs may contaminate the environment recipients such as soils, sediments, surface and underground water.⁷ Out of 16 ILs Petkovic et

al. identified that imidazolium ILs were the most toxic with cholinium-based ILs displaying significantly lower toxicity based on their effect on *Penicillium* genus fungi.⁸ Toxicity is also related to the lipophilic character of ILs. Peric et al. tested several kinds of soils with ILs and reported that ILs with longer alkyl chains such as $[C_8C_{1im}]Cl$ exhibited greater toxicity than ILs with smaller alkyl chains, for example $[C_4C_{1im}]Cl$. $[C_8C_{1im}]Cl$ was also found to adsorb more strongly to soil.⁹ Furthermore, Bernot et al. deduced that IL cations tend to contribute the most to the overall toxicity of ILs.¹⁰ Romero et al. revealed that anions also contribute to the toxicity of ILs. On investigating $[C_6C_{1im}]Cl$, $[C_6C_{1im}][PF_6]$, $[C_8C_{1im}]Cl$ and $[C_8C_{1im}][PF_6]$ ILs they identified that $[PF_6]$ was more toxic than Cl^- based on acute toxicity test on *V.fischeri* (*Photobacterium phosphoreum*).¹¹ ILs have also been tested for their toxicity to aquatic animals and fishes. The $[C_4C_{1im}][NTf_2]$, $[C_6C_{1im}][NTf_2]$ and $[C_4C_{1im}][HSO_4]$ ILs were tested for acute toxicity on fishes (*Cephalopholis cruentata* and *Poecilia reticulata*) which were kept in water with different IL concentrations. The mortality rate in fishes revealed that all of these ILs are practically not toxic to these fishes.⁵ Furthermore, Pernak et al. also studied the effects of alkoxy side chains and anions on the antimicrobial activity of imidazolium ILs.¹²

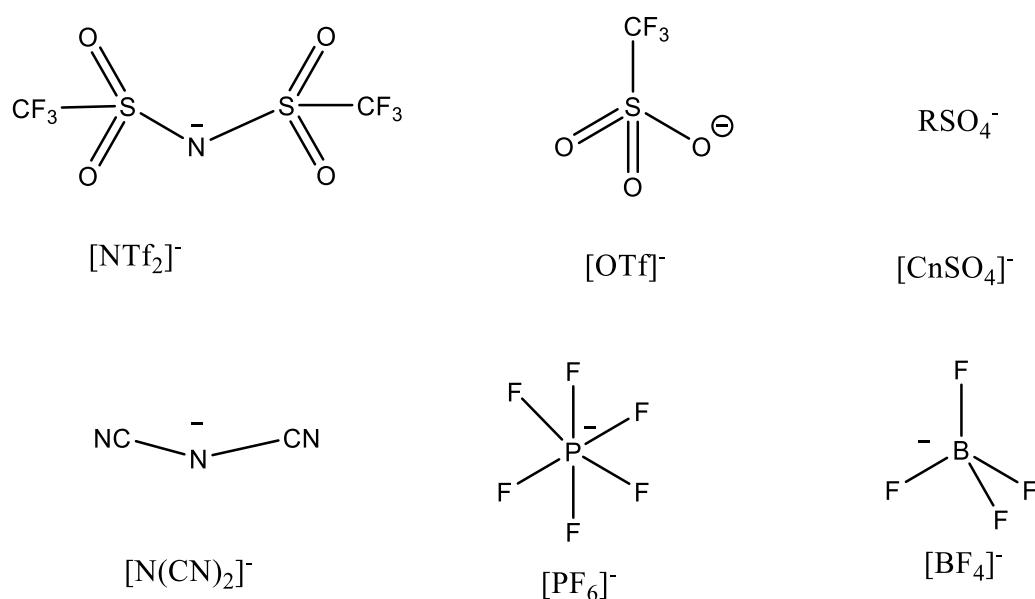


Figure 2. Common anions for ionic liquids (Adapted from Ref.⁶).

1.2. Classification of Ionic Liquids

ILs are classified on the basis of their chemical structure as either protic (proton donating) or aprotic (non-proton donating). Protic ILs (PILs) are usually produced through the proton transfer from a mixture of equal concentration of proton acceptor and proton donor.¹³ PILs possess higher conductivities and fluidity than structurally similar aprotic ionic liquids (AILs).¹⁴ Moreover, PILs possess less thermal stability and reduced ionicity at high temperature than aprotic ILs due to the reverse reaction of the proton that shifts the equilibrium towards the neutral constituents.¹⁵

In contrast, (AILs) do not have an acidic proton and are produced by the formation of a covalent bond to an atom other than hydrogen. As a result, their synthesis is usually not reversible and tends to completely form ions.¹³ Moreover, from molecular dynamics stimulations it has been demonstrated that the interactions between the ions in the AILs are less specifically oriented in contrast to PILs, which form well-defined hydrogen-bonding network.¹⁶ The aprotic ILs typically contain an additional alkyl chain with respect to protic ILs as shown in **Figure 3**.¹⁷

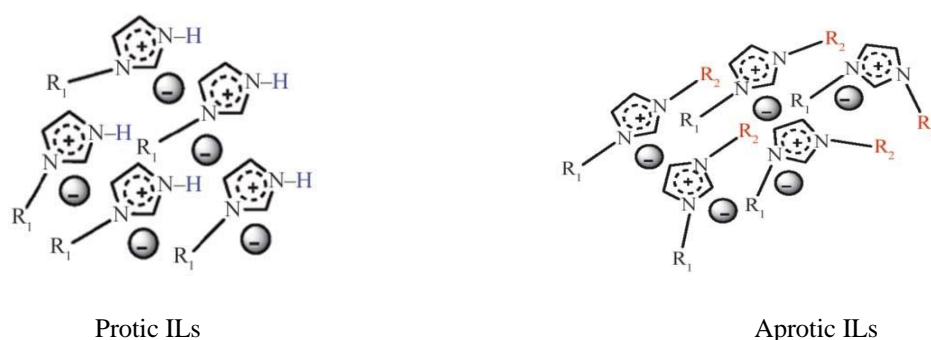


Figure 3. Structural arrangement of ions in protic and aprotic imidazolium ILs (Adapted from Ref.¹⁷).

Other IL classifications have been made based on structural qualities such as the presence of a chiral center, a divalent ion, a polymeric ion, a fluorocarbon moiety, amino acid IL, aromaticity and aryl alkyl ILs.¹³

1.3. Structure of Ionic Liquids

The structure of ILs involves the arrangement of strongly held ions of alternating charge as well as weaker directional interactions such as hydrogen bonding, dispersion forces and π -stacking interactions.¹³ The uniform arrangement of cations and anions in conventional high temperature molten salts comprising simple spherically symmetric ions, leads to large lattice

energies and hence high melting temperatures. **Figure 4** shows the arrangement of cations and anions in molten salts and ILs. Whereas, in ILs the organic cations are often larger in size and have low symmetry which stops them from crystallizing to make solids.¹⁷

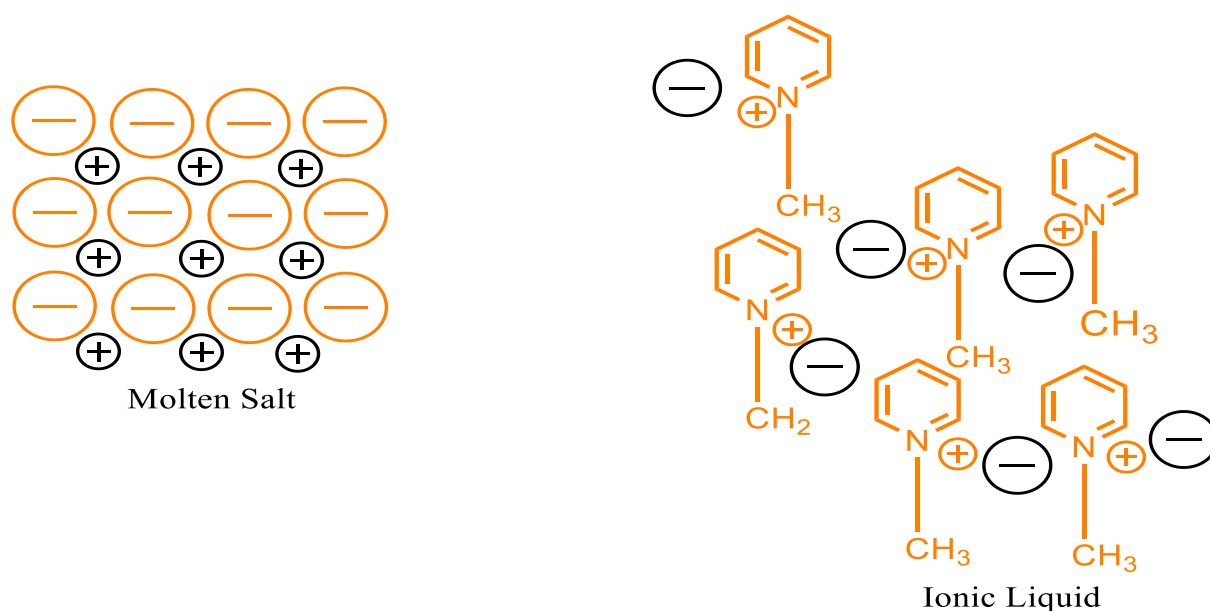


Figure 4. Arrangement of cations and anions in molten salts and ionic liquids. (Adapted from Ref.¹⁷).

The arrangement of ions in liquid phase is related to key physical characteristics including heat capacity and compressibility of the IL. The ion pairs are the replicating units evident in the bulk structure of ILs.¹³ However, ILs do not form well-defined ion pairs as has been demonstrated by exploring salts as solutes. It was found that ILs completely dissociate the cations and anions in the solute.¹⁸ Further evidence from NMR studies of IL mixtures indicated that there is no anion clustering around specific cations.¹⁹ Molecular dynamics have provided insight into the lifetime of specific ion-pairs through studies of H-bond lifetimes between specific ions. For imidazolium ILs, intermittent H-bonds were found to exist between similar ions for ≈ 5 ns before complete dissociation of the ion-pair, highlighting the short-lived nature of ion pairs within these solvents.²⁰

1.3.1. Hydrogen bonding

The hydrogen-bonding interactions in ILs was first proposed and clarified by Evans et al. in 1981 for ethylammonium nitrate. Weak molecular associations such as hydrogen bonding and

π -stacking imperative for the bulk structures seldom appear in molten salts. Whereas, in ILs such as $[\text{C}_n\text{C}_1\text{im}]^+$ cations connected with anions (Cl^- , SCN^-) both hydrogen bond and π -type interactions concurrently take place between the ions.²¹

IR spectra have been used to probe the existence and strength of hydrogen bonding interactions between ions.²² In 1994, NMR spectroscopy of $[\text{C}_2\text{C}_1\text{im}]\text{Cl}$ revealed that the $[\text{C}_2\text{C}_1\text{im}]^+$ cation form hydrogen bonds (through the three ring protons H^2 , H^4 , H^5) with halide ions in polar solvents.²³ The first FTIR measurements with $[\text{C}_2\text{C}_1\text{im}][\text{SCN}]$, $[\text{C}_2\text{C}_1\text{im}][\text{N}(\text{CN})_2]$, $[\text{C}_2\text{C}_1\text{im}][\text{EtSO}_4]$ and $[\text{C}_2\text{C}_1\text{im}][\text{NTf}_2]$ revealed the presence of hydrogen bonding evident from the change in the band shift with the varying anion due to the cation anion interaction. Within the aggregates the C2-H and C(4/5)-H involved in hydrogen bonds resulting in various frequencies and intensities.²⁴ Further, the existence of H-bonding in ILs is firmly apparent from X-ray, NMR and IR studies in the solid and liquid forms. In the case of imidazolium ILs the existence of H-bonding is marked by the small C-H---anion distances, red shifted C-H stretching in IR and C-H proton downfield shifting in NMR, particularly for the C-H bond in the 2-position of the imidazolium ring.²⁵ Quantum mechanics calculations have revealed that the most acidic hydrogen on the imidazolium ring, that in position-2 (**Figure 5**) account for the strongest formation of H-bonding with the anions. The hydrogens at positions 4 and 5 also engage in H-bonding but, not as strongly.²⁶

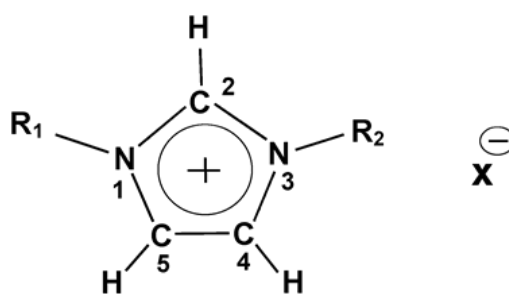


Figure 5. Position of H atoms on imidazolium ring (Adapted from Ref.²⁶).

As an example of the nature of hydrogen-bonding in imidazolium ILs, $[\text{C}_4\text{C}_1\text{im}]\text{Cl}$ has been widely studied **Figure 6** identifies possible association sites of the anion with the cation. In $[\text{C}_4\text{C}_1\text{im}]^+$, $\text{C}^2\text{-H}$ hydrogen bonding interactions are the most effective with H-Cl distance of 2 Å which is smaller than the combined Vander Waal radii of Cl and H of 2.95 Å. The weaker interactions around the ring can be seen in **Figure 6** and include $\text{C}^4\text{-H}$ and $\text{C}^5\text{-H}$. The hydrogen bonding in $\text{C}^4\text{-H}$ and $\text{C}^5\text{-H}$ bonds are influenced by steric effects arising from the long alkyl

chain. C-H groups adjacent to the imidazolium cation on the alkyl chain can also form supportive H-bonds with the anion, e.g. Figure 6 (3a).²⁷

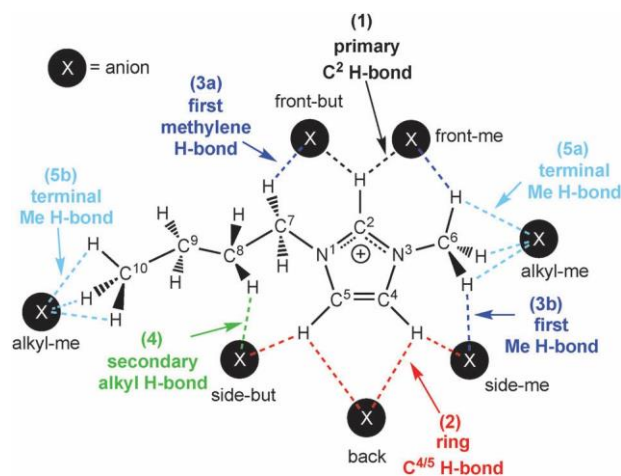


Figure 6. Imidazolium cation showing association sites for anion (Adapted from Ref.²⁷).

In the side-chain due to the greatest partial positive charge of the first carbon with the rest of the alkyl chain the C^7 -H and C^6 -H forms hydrogen bonds (3a and 3b in **Figure 6**) although these are even weaker again than the hydrogen bonds formed with the ring hydrogens. Many hydrogen bonding conformations have been observed with the anion interconnecting with $C^{6/7}$ -H and $C^{2/4/5}$ -H. The H-bond on ring are observed to be affected by the alkyl H-bond and make the anion move away from a linear orientation with respect to the $C^{2/4/5}$ -H positions.. The effect of alkyl H-bonds in the solution phase is determined by the vibrational redshift relative to the H-bonds of the calculated isolated gas-phase ion pairs, $\approx 650\text{cm}^{-1}$ for the C^2 -H, and ≈ 300 - 400cm^{-1} for coupled $C^{4/5}$ -H ring and alkyl $C^{6/7}$ -H.²⁸

1.3.2. Amphiphilic Nanostructure

ILs have strong coulombic and H-bonding interactions that result in the exclusion of the alkyl chains leading to the formation of polar and non-polar domains. The mesoscopic nanostructure of ILs was first proposed by Schroder et. al. related to the diffusion coefficient of three electrically active solutes dissolved into AILs.²⁹ It was deduced that IL-water mixtures form nanostructured solvents that contain polar and non-polar domains unlike common molecular solvents.¹³ In 2005, multiscale coarse-graining (MS-CG) simulations revealed the effect of the alkyl side chain length of cations in $[\text{C}_4\text{C}_{1\text{im}}][\text{NO}_3]$ IL. As the alkyl chain of cation is long, the alkyl tails form liquid crystal-like structures and affects the ILs properties such as their

structural dynamics and thermodynamic properties. Ionic channels are formed by the charged region rather than a homogenous organization of ions and alkyl chains as shown in **Figure 7**.³⁰

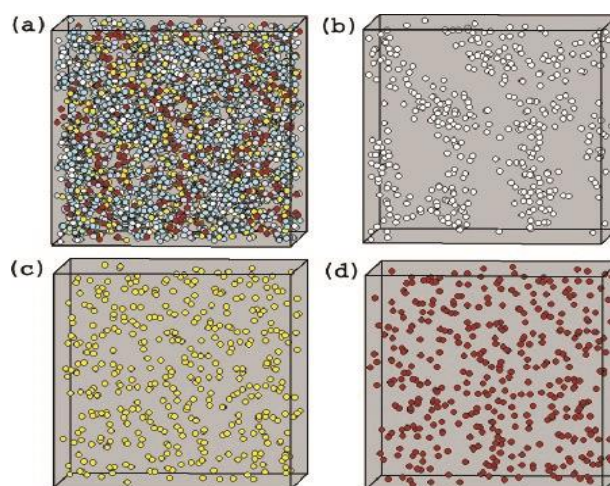


Figure 7. Structure of stimulation for ion pairs. (a) all atoms, (b) tail groups, (c) head groups only, and (d) anions only (Adapted from Ref.³⁰).

Further, the X-ray diffraction patterns from sequence of Cl salts at ambient temperature noted that [C₃mim]Cl shows no clear peaks whereas the remaining salts [C₄mim]Cl, [C₆mim]Cl, [C₈mim]Cl, [C₁₀mim]Cl display a peak which shifts position and increases in intensity with increasing alkyl chain length as shown in **Figure 8**. Moreover, the increase in spatial correlation (L) value with increasing alkyl chain length confirmed the formation of nanoscale non-polar domains comprising the IL alkyl chain.³¹

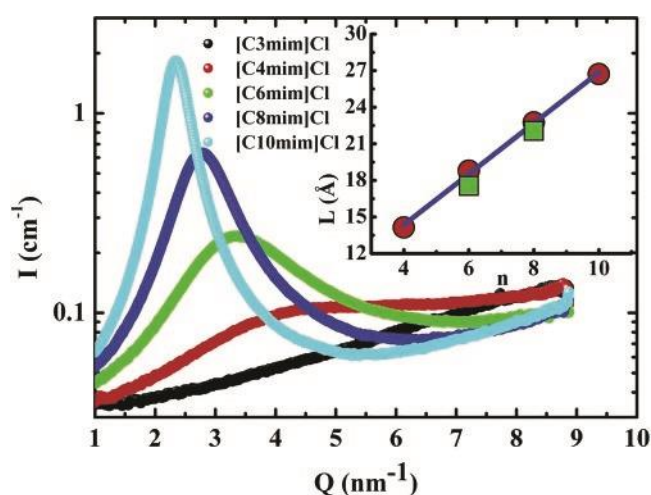


Figure 8. X-ray diffraction pattern from the series of RTILs: [C_nClim]Cl n=3,4,6,8,10 at 25°C. L= spatial correlation, n= the alkyl chain length. (Adapted from Ref.³¹).

For ILs containing short alkyl chains such as $[\text{C}_2\text{C}_1\text{mim}]^+$ ILs, a continuous phase is reported. Whereas, a sponge-like nanostructure with segregated polar and non-polar domains are observed in $[\text{C}_6\text{C}_1\text{mim}]^+$, $[\text{C}_8\text{C}_1\text{mim}]^+$ and, $[\text{C}_{12}\text{C}_1\text{mim}]^+$ ILs. $[\text{C}_4\text{C}_1\text{mim}]^+$ ILs act as display intermediate behavior whereas segregated domains can occur depends on the nature of anions **Figure 9**.¹³ The segregation of alkyl chains from the polar ionic networks has been proposed to arise from strong electrostatic forces between IL anions and the van-der-Waals forces between the aggregated alkyl chains.³²

From the X-ray scattering data is also revealed that the increase or decrease in nano-segregation with the increase in alkyl chain is also temperature dependent that is different in alkyl chains.³³

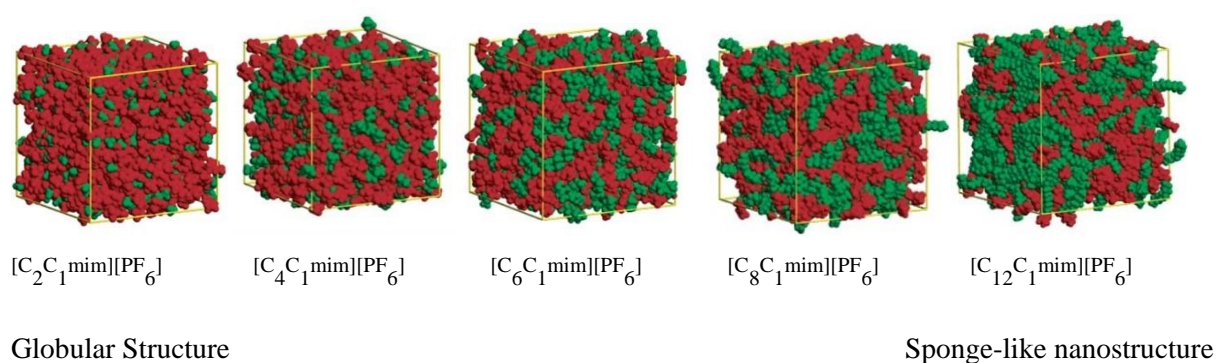


Figure 9. Bulk structure of $[\text{C}_n\text{C}_1\text{mim}][\text{PF}_6]$ with $n=2-12$ (Adapted from Ref.¹³).

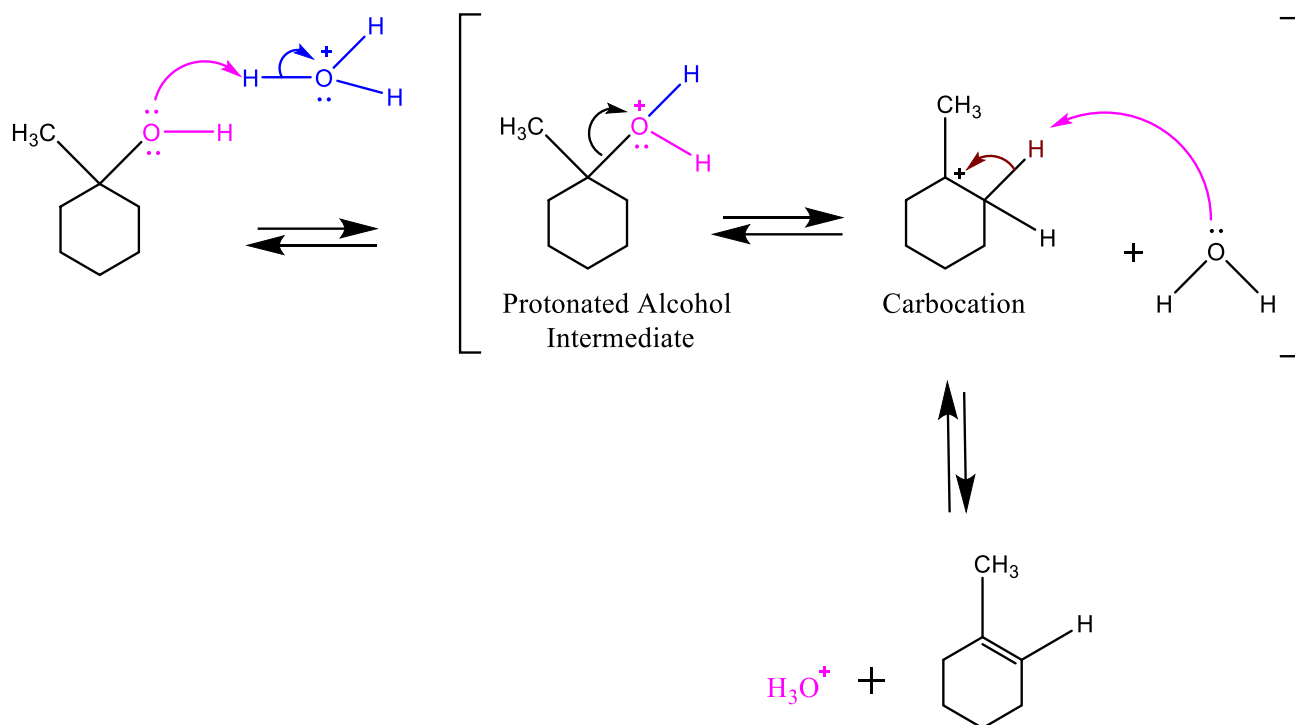
Chain functionalisation is an important factor influencing the formation of segregated nanoscale domains. It was observed that the presence of a hydroxyl or ether group enhanced the polarity of the side chains, eliminating the formation of mesoscopic order even for side chains containing functional groups.³⁴

1.4. Alcohol Dehydration Mechanism

The dehydration of alcohols to form alkenes mainly proceeds via an acid catalyzed elimination reaction. This leads to a net loss of H_2O from the breaking of a C-OH and C-H bond, resulting in π bond formation. The reactivity of alcohols towards elimination increases in the order primary < secondary < tertiary alcohols.³⁵

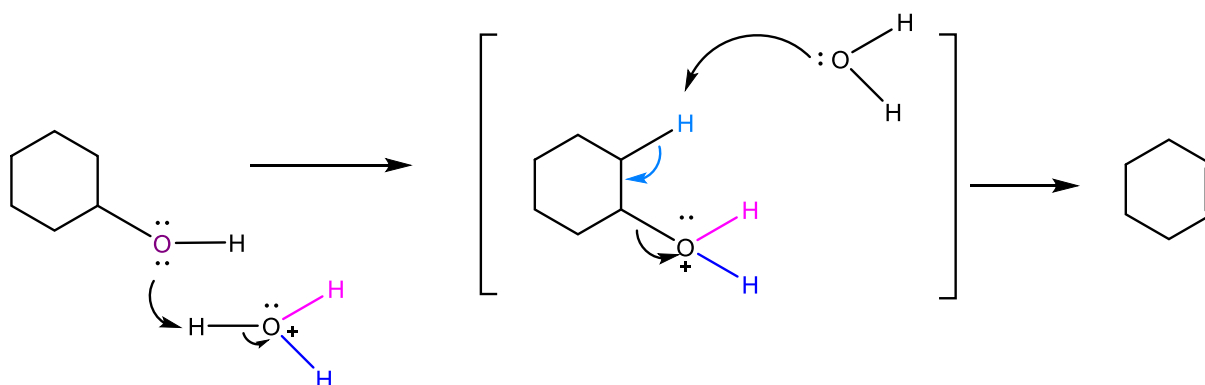
Dehydration of alcohol can take place by two main mechanisms, E_1 and E_2 reactions. E_1 reactions involve three steps including protonation of the alcohol oxygen, the loss of water leading to a carbocation intermediate and the subsequent ultimate loss of the proton from the neighboring carbon atom to form the π bond (**Scheme 1**). The rate determining step is the

unimolecular loss of water from the protonated intermediate. Tertiary and secondary alcohols dehydrate primarily through an E₁ mechanism whereas the carbocation intermediate for primary alcohols is too unstable to proceed through this mechanism.³⁵



Scheme 1. E₁ Reaction (Adapted from Ref.³⁵).

E₂ mechanisms involve a synchronous loss of water and attack by a base on the α-proton. This pathway is common for primary alcohols. In E₂ elimination, another water molecule attacks the proton on the adjacent carbon and simultaneously a cycloalkene is formed in one step (**Scheme 2.**)³⁵



Scheme 2. E₂ reaction mechanism.

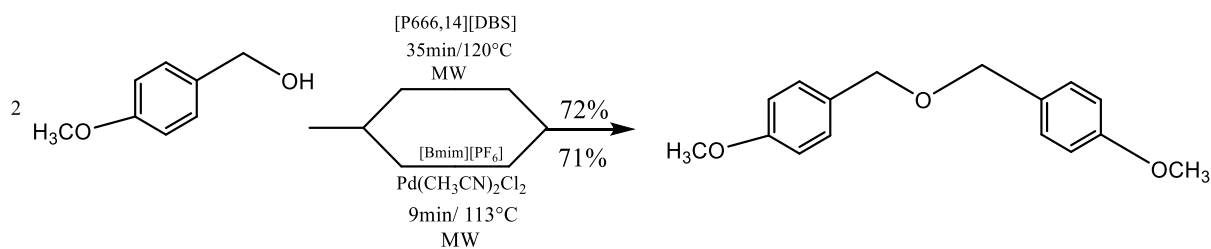
Acid-catalysed reactions of alcohols can also produce ethers along with the alkenes. This can occur from the addition of another molecule of alcohol to the alkene or from the nucleophilic attack of the alcohol on the carbocation intermediate.³⁶

1.5. Alcohol Dehydration In Ionic Liquids

Alcohol dehydration reactions encompass both substitution and elimination reactions. Substitution reactions can be utilized in a large variety of conversions such as esterification, etherification, and thioetherification whereas elimination form alkenes or carbonyl groups in the case of diols or polyols. Similarly, the etherification of primary and benzyl alcohol with *p*-toluene sulfonic acid (TsOH) gave traces of products while with dodecylbenzenesulfonic acid (DBSA) yields higher amount of ethers as products.³⁷ The microwave irradiation of benzyl alcohol to form dibenzylether using Pd(CH₃CN)₂Cl₂ as a catalyst in the ILs [C₄C₁im][PF₆], [C₄C₁im][BF₄], [C₄C₁im] was studied by Kalviri et. al.³⁸ 55% dibenzylether was reported with [C₄C₁im][PF₆] under microwave irradiation for seven minute. The deterioration of [C₄C₁im][PF₆] was evident from the development of a precipitate after extended heating arising from HF product due to the decomposition of the PF₆ anion.³⁹

The microwave irradiation of 4-methoxyphenylpropan-1-ol in the presence of [C₄C₁im]Cl, [C₄C₁im][PF₆], [C₄C₁im][BF₄], [C₄C₁im]Br and, [C₆C₁im]Br lead to the formation of 4-methoxyphenylpropene with the highest yield obtained for [C₆C₁im]Br. Whether any structural effects arising from the longer alkyl side chains of this IL played an important role in its reactivity remains unknown since only one IL with a longer alkyl chain was explored.⁴⁰

Ether formation was reported from 4-methoxybenzyl alcohol (4-MBA) in the presence of IL trihexyl-tetradecylphosphonium dodecylbenzene sulfonate, [P_{666,14}][DBS] and [C₄C₁im][PF₆] in the presence and absence of Pd(CH₃CN)₂Cl₂ under MW conditions was investigated. Moreover, [P_{666,14}][DBS] was able to achieve similar yields to [C₄C₁im][PF₆] under comparable conditions but in the absence of metal catalyst as shown in **Scheme 3**.³⁸



Scheme 3. 4-methoxybenzyl alcohol etherification dehydration in [P_{666,14}][DBS] and [C₄C_{1im}][PF₆] (Adapted from Ref.³⁸).

In the case of the reaction with the Pd catalyst the product decays with prolonging heating. Whereas, without Pd the product yield increases until saturation. The rate was found to increase with the increase in the water concentration in the reaction mixture. Furthermore, at several concentrations of 4-methoxybenzyl alcohol a higher yield was obtained with a higher concentration of IL as the reaction was found to be first order in [P_{666,14}][DBS] (**Table 1**). The NMR and elemental studies demonstrated the absence of acidic impurities in the phosphonium ILs. In the case of secondary benzylic alcohol dehydration in [P_{666,14}][DBS] and other [P_{666,14}]⁺ ILs based on halide anions (Cl⁻, Br⁻), the alkene was obtained as the major product.³⁸

Table 1. Results from ¹HNMR spectroscopy with mesitylene or acetophenone as standards (Adapted from Ref³⁸).

Entry	Substrate	Alkene	Ionic Liquid	Yield (%)	Time (min)/Temp. [°C]
1			[P _{666,14}][DBS]	96	30/120
2			[P _{666,14}][Br]	99	30/120
3			[P _{666,14}][Cl]	30	30/120

1.6. Project Aim

There have been only seen a few examples of ILs acting as solvents and catalysts for the dehydration of alcohols, a class of reactions of growing importance due to the ability to convert carbohydrates obtained from biomass. None of these studies has clearly identified the specific role of the IL anion or the amphiphilic nanostructure of the IL. Hence, the aim of this project is to explore the effect of the amphiphilic nanostructure and nature of the IL anion on the rate and selectivity of model alcohol dehydration reactions to enable the future rational design of optimal solvent systems for these transformations. By not using an added acid catalyst, the aim is to identify the specific role of the IL itself, if any, in these transformations.

The major question this thesis aims to address is:

- How does the existence and absence of nanostructure in ILs affect the reactivity of alcohols when the IL is used as a solvent?
- How does the general structure of the IL influence the dehydration of alcohols in the absence of a strong acid catalyst?
- Can the selectivity for ethers over alkenes be affected by the choice of ILs?

1-alkyl-3-methylimidazolium ILs will be the focus of this study due to their availability, widespread use within the IL community and extensive studies on their ability to form amphiphilic nanostructures.

CHAPTER 2: EXPERIMENTAL

2.1. General

The following chemicals were used as received: octan-2-ol (Merck, 98%), octan-1-ol (BDH Laboratory Reagents, 95%), tert-Amyl alcohol (Sigma-Aldrich, 99%), cyclohexanol (Merck), cyclohexene (Sigma Aldrich, 99%), cyclohexanone (Acros Organics, 99.8%), oct-1-ene (Sigma-Aldrich), mesitylene (Merck, 98%), dry silica gel (Merck), dichloromethane (Merck, 99.8%), n-hexane (Sigma Aldrich, 95%), diethyl ether (Merck), ethyl acetate (Merck), trans-2-octene, trans-1-octene and 1,4-cyclohexandiol. 1-Methylimidazole, 1-chlorodecane, 1-chlorooctane were distilled under reduced pressure. 1-Chlorohexane was distilled under a nitrogen atmosphere before use. The ILS $[\text{C}_{10}\text{C}_{1\text{im}}]\text{Cl}$, $[\text{C}_8\text{C}_{1\text{im}}]\text{Cl}$, $[\text{C}_6\text{C}_{1\text{im}}]\text{Cl}$, $[\text{C}_{10}\text{C}_{1\text{im}}][\text{NTf}_2]$, $[\text{C}_{10}\text{C}_{1\text{im}}][\text{Me}_2\text{PO}_4]$, $[\text{C}_{10}\text{C}_{1\text{im}}][\text{OTf}]$, $[\text{C}_6\text{C}_{1\text{im}}][\text{OTf}]$, $[\text{C}_8\text{C}_{1\text{im}}][\text{OTf}]$, $[\text{C}_8\text{C}_{1\text{im}}][\text{NTf}_2]$, $[\text{C}_6\text{C}_{1\text{im}}][\text{NTf}_2]$ were synthesized according to the experimental procedures described below and dried at 55°C-65°C in vacuo before use. The $[\text{C}_{10}\text{C}_{1\text{im}}]\text{Br}$ and $[\text{C}_2\text{C}_{1\text{im}}][\text{NTf}_2]$, $[\text{C}_4\text{C}_{1\text{im}}][\text{NTf}_2]$, $[\text{C}_4\text{C}_{1\text{im}}][\text{OTf}]$ was synthesized by the other members of Weber group. Methanol and acetonitrile (Analytical Reagent) were dried with activated molecular sieves for 12 hours before use in reactions.

2.2. Physical Measurements

2.2.1. NMR

^1H , ^{13}C , ^{19}F and ^{31}P NMR spectra were recorded on a Bruker Ascend 400MHz NMR Spectrometer at ambient temperature. The measurement frequencies for ^1H , ^{13}C , ^{19}F and ^{31}P NMR were 400 MHz, 101MHz, 376 MHz and, 162 MHz respectively. The solvents used in NMR measurements were deuterated dimethyl sulfoxide ($\text{DMSO-}d_6$) and chloroform (CDCl_3). Chemical shifts were referenced to residual solvent peaks.

2.2.2. Gas Chromatography with Flame Ionization Detector (GC-FID)

Gas chromatography analysis was performed on a Shimadzu GC-FID 2010 Plus equipped with a DB-FATWAX UI column and flame ionization detector.

2.2.3. Method for GC-FID Analysis

The analysis of 2-octanol and cyclohexanol reaction mixtures was performed using a 29 minute programme with a 1 μL injector volume, split ratio of 40 and injector temperature of 250°C.

The oven temperature was initially held at 50 °C then heated at a rate of 10°C min⁻¹ then held at 230°C for a further 3 minutes.

2.2.4. Method for GC-MS Analysis

The samples were analysed using the Agilent 7890A GC equipped with 5977A mass spectrometer detector (MSD) with an Electron Impact ionisation source. The separation was achieved by Agilent HP-5ms UI column (30m x 0.25mm x 0.25µm). The inlet temperature was set at 265 °C and the samples were injected in pulsed split mode with a split ratio of 50:1. The initial column temperature was held at 50 °C for 8 minutes and then ramped at 10 °C/min to 230 and held for 3 minutes. MSD transfer line was held at 250 °C, ion source at 230 °C and the quad at 150 °C. The data were acquired in 29 minutes with 2 minutes solvent delay in the mass range 37-500 Da.

2.2.5. Analysis by ICP-MS

The samples for ICP-MS was analysed on Agilent 7700 ICP-MS with an x-lens. No reaction gas was used in the cell because Lithium ($m/z = 7$) does not suffer from any spectral interferences. The ILs containing [NTf₂] as an anion was analyzed by Inductively Coupled Plasma Mass Spectrometry Agilent 7700 ICP-MS. 1000ppm dilution of IL firstly dissolved in 5 mL ACN and dissolved in 3% HNO₃.

2.3. General Procedures

2.3.1. Dehydration of alcohols

The general procedure for the dehydration reactions of alcohols involve heating a mixture of mesitylene (internal standard, 20 wt% relative to alcohol), alcohol and IL at the desired temperature between 70-180°C. After the completion of the reaction, it was quenched by placing the reactor in an ice bath for an hour. The reaction products were then separated by one of the extraction methods described below and the products analysed by GC-FID.

2.3.1.1. Extraction of products by using column chromatography

The IL from the reaction mixture was removed by column chromatography using a pipette column loaded with silica eluted with dichloromethane. The volume of the sample varied from 0.25mL to 1.5mL in order to determine the most efficient separation. The presence of IL in the

dichloromethane was determined by ^1H NMR analysis. This was used to inform the number of fractions that could be collected without IL breakthrough. Products isolated were quantified by GC-FID.

2.3.1.2. Extraction of products using solvent extraction

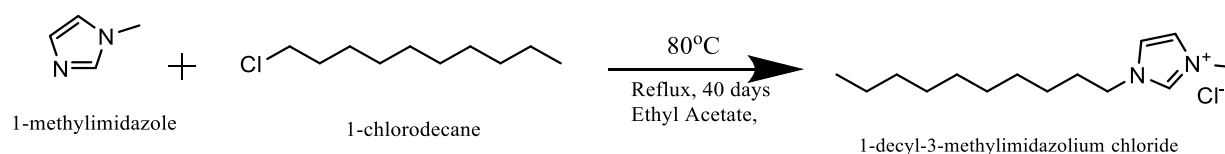
The products formed according to **procedure 2.3.1** were separated by the extraction of the reaction mixture with hexane. Depending on the miscibility of products either 10 drops of the reaction mixture or the entire reaction mixture was extracted with hexane. If 10 drops were used these were extracted with 2 mL \times 10 or 15 times hexane. The full reaction mixture was extracted with, 5 mL \times 10times of hexane. A small sample of the reaction mixture prior to reaction was extracted with hexane (2 mL \times 10 times) to determine the recovery of starting material that could be achieved. The IL layer was checked for the presence of reactants and products with ^1H NMR. The extracted hexane layers were combined and analyzed by GC-FID.

2.3.2. GC-FID Calibration

To calibrate the GC-FID for cyclohexanol and the major expected products, mesitylene: cyclohexanol: cyclohexanone: cyclohexene were accurately weighed into five vials with mass ratios of 1:5:5:5, 1:2:2:2, 1:1:1:1, 2:1:1:1 and, 5:1:1:1 respectively. These solutions were dissolved in 1mL of hexane with further dilution of 10 μ L of this solution to 1mL with hexane. These were quantified using GC-FID to establish calibration curves.

2.4. Synthesis of Ionic Liquids

2.4.1. Synthesis of 1-decyl-3-methylimidazolium chloride [$\text{C}_{10}\text{C}_{1}\text{im}$] Cl



Scheme 4. Synthesis of [$\text{C}_{10}\text{C}_{1}\text{im}$] Cl

Using the procedure described in Weber et al.⁴¹ 1-methylimidazole (25.74 g, 0.312 moles) was dissolved in approximately 80mL of ethyl acetate and 1-chlorodecane (58 g, 0.328 mol, 1.05

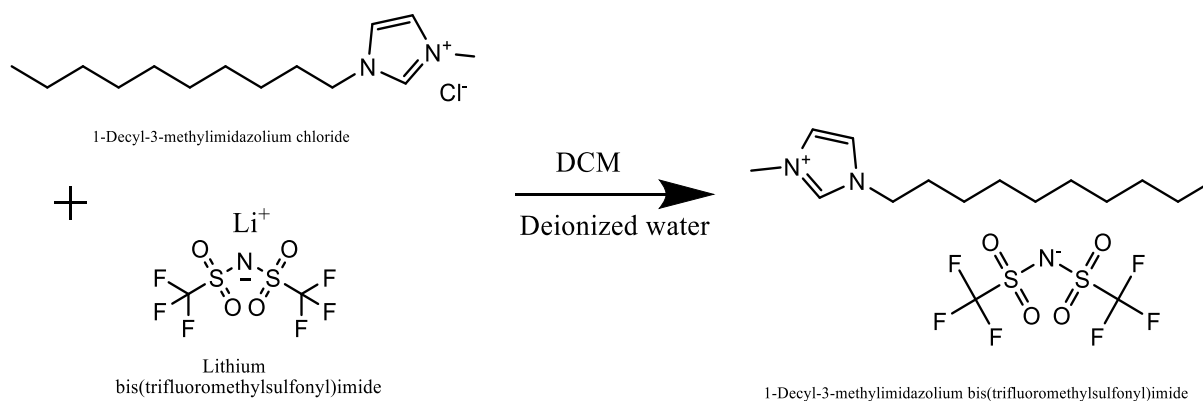
equiv.) was added slowly at room temperature with continuous stirring. The resultant solution was heated to reflux at 80°C with continuous stirring for 40 days. On completion of the reaction ethyl acetate was removed by rotary evaporation and the resultant liquid washed with diethyl ether (26 x 200 mL) to remove residual 1-methylimidazole. The resultant liquid was dried in high vacuum to yield [C₁₀C₁im] Cl as a pale-yellow liquid.

Yield: 62.6 g, 0.2419 mol, 77%

¹H NMR (400 MHz, DMSO-d₆): δ(ppm)= 9.09 (s, 1H), 7.75 (t, *J* = 1.8 Hz, 1H), 7.69 (t, *J* = 1.7 Hz, 1H), 4.15 (t, *J* = 7.2 Hz, 2H), 3.85 (s, 3H), 1.83 – 1.72 (m, 2H), 1.25 (s, 14H), 0.86 (t, *J* = 6.9 Hz, 3H).

¹³C {¹H} NMR (101 MHz, DMSO-d₆): δ(ppm)= 136.94 (s), 124.06 (s), 122.71 (s), 118.36 (s), 49.26 (s), 36.18 (s), 31.73 (s), 29.83 (s), 29.34 (s), 29.26 (s), 29.11 (s), 28.81 (s), 25.94 (s), 22.53 (s), 14.35 (s).

2.4.2. Synthesis of 1-decyl-3-methylimidazolium bis(trifluoromethanesulfonyl)imide [C₁₀C₁im][NTf₂]



Scheme 5. Synthesis of [C₁₀C₁im][NTf₂]

Using the procedure described in Weber et al.⁴¹ 1-Decyl-3-methylimidazolium chloride (15.86 g, 0.0613 mol) and lithium bis(trifluoromethylsulfonyl)imide (18.49 g, 0.0644 mol, 1.05 equiv.) were separately dissolved in 100 mL deionized water and then combined. 150 mL of DCM was added to extract the IL. The DCM was washed with deionized water (4×100 mL) until the absence of halide was confirmed with concentrated silver nitrate solution. The DCM was removed by rotary evaporator and the resultant liquid dried in vacuo at 55°C to yield [C₁₀C₁im] [NTf₂] as a clear colorless liquid.

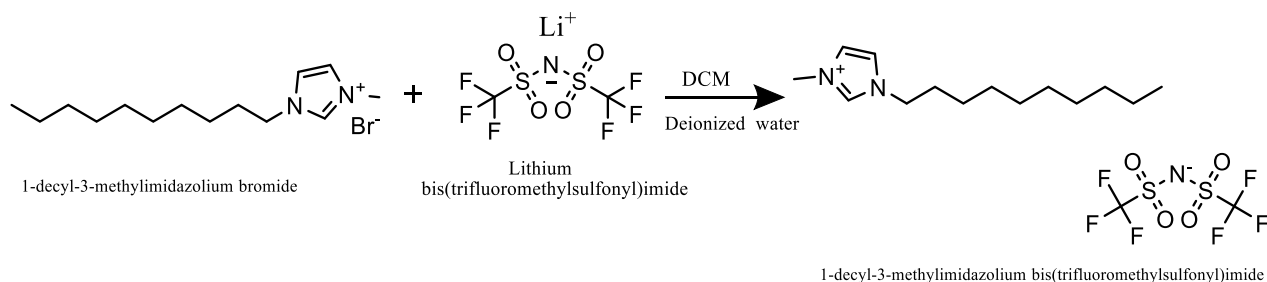
Yield: 25.5 g, 0.0506 mol, 83%

¹H NMR (400 MHz, DMSO-*d*₆): δ(ppm)= 9.09 (s, 1H), 7.75 (t, *J* = 1.8 Hz, 1H), 7.69 (t, *J* = 1.7 Hz, 1H), 4.15 (t, *J* = 7.2 Hz, 2H), 3.85 (s, 3H), 1.83 – 1.72 (m, 2H), 1.25 (s, 14H), 0.86 (t, *J* = 6.9 Hz, 3H).

¹³C {¹H} NMR (101 MHz, DMSO-*d*₆): δ(ppm)= 136.47 (s), 123.59 (s), 122.25 (s), 119.47 (q, *J* = 323 Hz), 48.76 (s), 35.72 (s), 31.25 (s), 29.35 (s), 28.87 (s), 28.79 (s), 28.63 (s), 28.34 (s), 25.46 (s), 22.06 (s), 13.91 (s).

¹⁹F NMR (376 MHz, DMSO-*d*₆): δ(ppm)= -78.72 (s, CF₃).

2.4.3. Synthesis of 1-decyl-3-methylimidazolium bis(trifluoromethanesulfonyl)imide [**C**₁₀**C**₁**im**][**NTf**₂]



Scheme 6. Synthesis of [C₁₀C₁im][NTf₂]

Using the procedure described in Weber et al.⁴¹ 1-Decyl-3methylimidazolium bromide (15.0 g, 0.0494 mol) and lithium bis(trifluoromethylsulfonyl)imide (14.93 g, 0.0520 mol, 1.05 equiv.) dissolved separately in 100 mL of deionized water and then mixed together. 150 mL of DCM was added to extract the IL. The DCM was washed with deionised water (4×100 mL) until the halide was confirmed to be absent using 0.1M AgNO₃ solution. The DCM removed by rotary evaporator and the resultant liquid dried in vacuo at 60°C to yield [C₁₀C₁im] [NTf₂] as a clear colorless liquid.

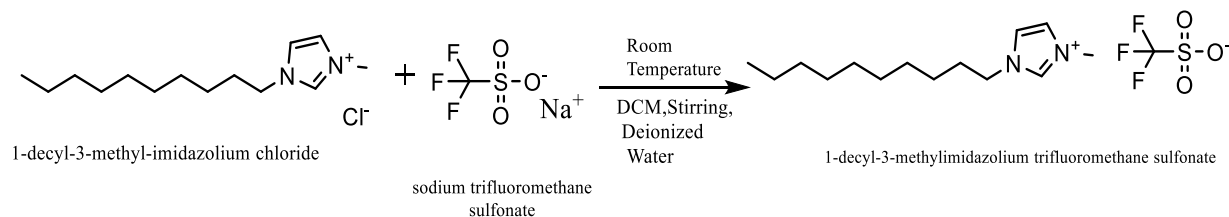
Yield: 23.7 g, 0.0471 mol, 95%

¹H NMR (400 MHz, DMSO-*d*₆): δ(ppm)= 9.09 (s, 1H), 7.76 (t, *J* = 1.8 Hz, 1H), 7.69 (t, *J* = 1.8 Hz, 1H), 4.14 (t, *J* = 7.2 Hz, 2H), 3.84 (s, 3H), 1.85 – 1.70 (m, 2H), 1.33 – 1.16 (m, 14H), 0.90 – 0.81 (m, 3H).

¹³C {¹H} NMR (101 MHz, DMSO-*d*₆): δ(ppm)= 136.47 (s), 123.59 (s), 122.24 (s), 119.47 (q, *J* = 323 Hz), 48.76 (s), 35.71 (s), 31.25 (s), 29.35 (s), 28.86 (s), 28.78 (s), 28.63 (s), 28.33 (s), 25.46 (s), 22.06 (s), 13.90 (s).

¹⁹F NMR (376 MHz, DMSO-*d*₆): δ(ppm)= -78.72 (s).

2.4.4. Synthesis of 1-decyl-3-methylimidazolium trifluoromethanesulfonate [C₁₀C₁im][OTf]



Scheme 7. Synthesis of [C₁₀C₁im][OTf]

Using the procedure described in Brooks et al.⁴² Sodium trifluoromethane sulfonate (10.86 g, 0.0631 mol, 1.09 equiv.) was suspended in a solution of 1-decyl-3-methylimidazolium chloride (15.04 g, 0.0580 mol) and DCM (150 mL). The slurry was stirred for 72 hours and filtered. The filtrate was washed with water (10 mL \times 4) until no halide could be detected with concentrated silver nitrate solution. The solvent removed by rotary evaporator and resultant liquid dried in vacuo at 60°C to yield [C₁₀C₁im][OTf] as a pale yellow liquid.

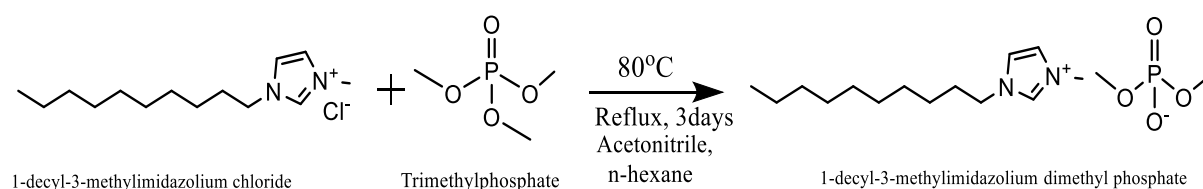
Yield: 19.4 g, 0.0521 mol, 90%

¹H NMR (400 MHz, DMSO-d₆): δ (ppm)= 9.10 (s, 1H), 7.77 (t, J = 1.8 Hz, 1H), 7.71 (t, J = 1.7 Hz, 1H), 5.99 (s, 1H), 5.80 – 5.72 (m, 2H), 5.54 (s, 1H), 4.16 (t, J = 7.2 Hz, 2H), 3.86 (s, 3H), 1.85 – 1.71 (m, 2H), 0.87 (t, J = 8.2, 5.6 Hz, 3H).

¹³C {¹H} NMR (101 MHz, DMSO-d₆): δ (ppm)= 136.46 (s), 123.60 (s), 122.25 (s), 54.89 (s), 48.76 (s), 35.73 (s), 31.25 (s), 29.35 (s), 28.83 (s), 28.64 (s), 28.34 (s), 25.47 (s), 22.07 (s), 13.93 (s).

¹⁹F NMR (376 MHz, DMSO-d₆): δ (ppm)= -77.76 (s).

2.4.5. Synthesis of 1-decyl-3-methylimidazolium dimethylphosphate [C₁₀C₁im][Me₂PO₄]



Scheme 8. Synthesis of [C₁₀C₁im][Me₂PO₄]

Using the procedure described in Yalcin et al.⁴³ 1-Decyl-3-methylimidazolium chloride (23.66 g, 0.0914 moles), was dissolved in 95 mL acetonitrile. Trimethyl phosphate (18.92 g, 0.1351 moles, 1.5 equiv.) was added to this solution and the solution was heated to reflux at 80°C for 3 days. As chloride was still present the resultant solution was stirred at the same temperature under nitrogen for 4 more days to aid the removal of chloromethane. As chloride was still present after a further 4 days, additional trimethylphosphate (12.64 g, 0.0902 moles, 1 equiv) was added to the reaction mixture. The reaction continued for 3 days at 80°C and stirred until the absence of chloride was confirmed by testing with concentrated silver nitrate solution. The solvent was removed by rotary evaporator and the resultant liquid was washed with n-hexane (30×100mL). The resultant IL was dried in vacuo at 55°C to yield [C₁₀C₁im] [Me₂PO₄] as a pale-yellow liquid.

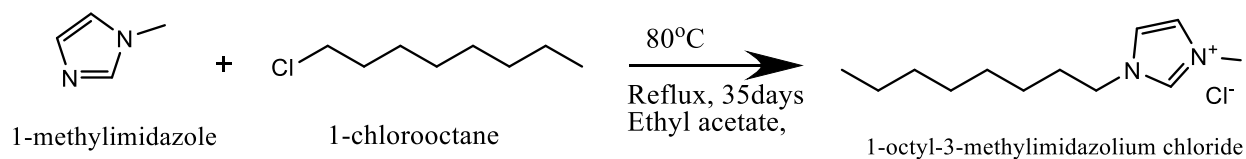
Yield: 17.11 g, 0.0491 mol, 54%.

¹H NMR (400 MHz, DMSO-d₆): δ(ppm)= 9.35 (s, 1H), 7.80 (t, *J* = 1.7 Hz, 1H), 7.73 (t, *J* = 1.7 Hz, 1H), 4.16 (t, *J* = 7.2 Hz, 2H), 3.86 (s, 3H), 1.83 – 1.72 (m, 2H), 1.24 (s, 14H), 0.86 (t, *J* = 6.8 Hz, 3H).

¹³C {¹H} NMR (101 MHz, DMSO-d₆): δ(ppm)= 136.89 (s), 123.58 (s), 122.26 (s), 51.25 (d, *J* = 5.9 Hz), 48.70 (s), 35.65 (s), 31.26 (s), 29.40 (s), 28.88 (s), 28.81 (s), 28.64 (s), 28.37 (s), 25.49 (s), 22.07 (s), 13.92 (s).

³¹P NMR (162 MHz, DMSO-d₆): δ(ppm) = 1.10 (sep, *J* = 10.2 Hz).

2.4.6. Synthesis of 1-octyl-3-methylimidazolium chloride [C₈C₁im]Cl



Scheme 9. Synthesis of [C₈C₁im]Cl

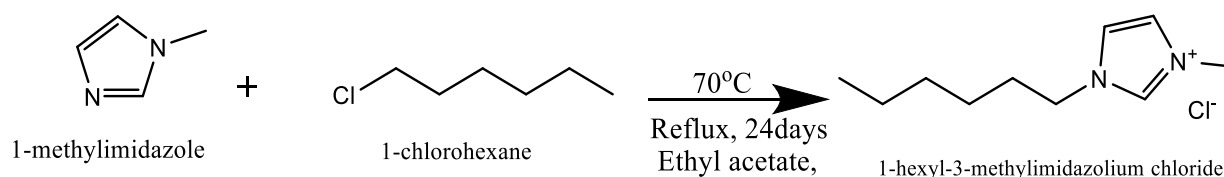
Using the procedure described in Weber et al.⁴¹ 1-methylimidazole (50.01 g, 0.6091 mol) was dissolved in ethyl acetate (160 mL) and 1-chlorooctane (86.35 g, 0.5808 mol, 1.05 equiv.) added slowly to this solution with continuous stirring. The mixture was heated to reflux at 80°C for 35 days. The solvent was removed, and the resultant IL washed with diethyl ether (40×100 mL). IL obtained was dried in vacuo at 60°C to yield [C₈C₁im]Cl as a clear colorless liquid.

Yield: 100.74 g, 0.4365 mol, 72%.

^1H NMR (400 MHz, DMSO- d_6): $\delta(\text{ppm})= 10.23$ (s, 1H), 9.27 (s, 1H), 7.81 (t, $J = 1.8$ Hz, 1H), 7.74 (t, $J = 1.7$ Hz, 1H), 4.18 (t, $J = 7.2$ Hz, 2H), 3.87 (s, 3H), 1.85 – 1.72 (m, 2H), 1.34 – 1.19 (m, 10H), 0.90 – 0.83 (m, 3H).

^{13}C $\{^1\text{H}\}$ NMR (101 MHz, DMSO- d_6): $\delta(\text{ppm})= 136.60$ (s), 123.58 (s), 122.25 (s), 48.72 (s), 35.71 (s), 31.14 (s), 29.38 (s), 28.39 (s), 25.48 (s), 22.03 (s), 13.92 (s).

2.4.7. Synthesis of 1-hexyl-3-methylimidazolium chloride [$\text{C}_6\text{C}_{1\text{im}}\text{Cl}$]



Scheme 10. Synthesis of [$\text{C}_6\text{C}_{1\text{im}}\text{Cl}$]

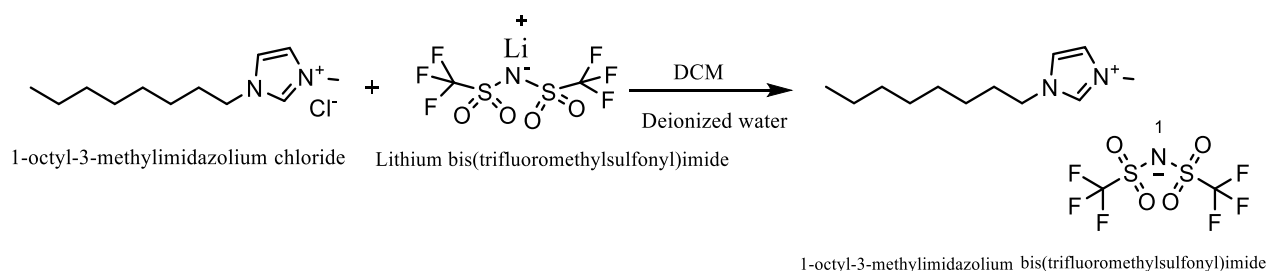
Using the procedure described in Weber et al.⁴¹ 1-Chlorohexane (60.37 g, 0.5047 moles, 1.05 equiv.) was added dropwise to 1-methylimidazole (43.48 g, 0.5296 moles) dissolved in 140 mL of ethyl acetate at room temperature with constant stirring. The resultant solution was heated to 70°C for 24 days. The solvent was evaporated on rotary evaporator and the resultant liquid washed with diethyl ether (60×100 mL). The diethyl ether was removed by rotary evaporator and the resultant IL was dried in vacuum at 60°C to yield [$\text{C}_6\text{C}_{1\text{im}}\text{Cl}$] as a pale-yellow liquid.

Yield: 87.1 g, 0.4295 mol, 81%.

^1H NMR (400 MHz, DMSO- d_6): $\delta(\text{ppm})= 9.43$ (s, 1H), 7.85 (t, $J = 1.8$ Hz, 1H), 7.78 (t, $J = 1.7$ Hz, 1H), 4.19 (t, $J = 7.2$ Hz, 2H), 3.88 (s, 3H), 1.85 – 1.70 (m, 2H), 0.91 – 0.79 (m, 3H).

^{13}C $\{^1\text{H}\}$ NMR (101 MHz, DMSO- d_6): $\delta(\text{ppm})= 136.63$ (s), 123.58 (s), 122.25 (s), 48.70 (s), 35.71 (s), 30.53 (s), 29.34 (s), 25.12 (s), 21.85 (s), 13.82 (s).

2.4.8. Synthesis of 1-octyl-3-methylimidazolium bis(trifluoromethylsulfonyl)imide [C_8C_1im][NTf_2]



Scheme 11. Synthesis of [C_8C_1im][NTf_2]

Using the procedure described in Weber et al.⁴¹ 1-Octyl-3methylimidazolium chloride (15.14 g, 0.0656 moles) and, lithium bis(trifluoromethylsulfonyl)imide (19.78 g, 0.0689 moles, 1.05eq) were separately added to 100 mL of deionized water. Both the solutions were then combined, and 150 mL of DCM was added to it. The organic phase was washed with deionized water (4×100 mL) until the absence of halide was confirmed with concentrated silver nitrate solution. The DCM was evaporated by rotary evaporator and the resultant liquid dried on high vacuum at 55°C to yield [C_8C_1im] [NTf_2] as a clear colorless liquid.

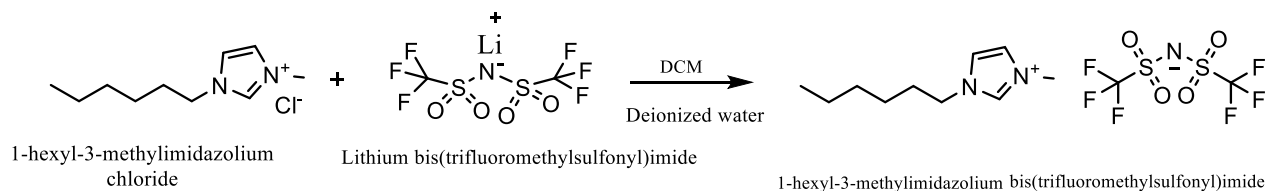
Yield: (29.9 g, 0.0629 mol, 96%)

1H NMR (400 MHz, DMSO- d_6): δ (ppm)= 9.11 (s, 1H), 7.77 (t, J = 1.8 Hz, 1H), 7.70 (t, J = 1.7 Hz, 1H), 4.16 (t, J = 7.2 Hz, 2H), 3.86 (s, 3H), 1.85 – 1.73 (m, 2H), 1.29 (m, 10H), 0.92 – 0.83 (m, 3H).

^{13}C { 1H } NMR (101 MHz, DMSO- d_6): δ (ppm)= 136.47 (s), 123.60 (s), 122.25 (s), 119.48 (q, J = 324 Hz), 48.77 (s), 35.72 (s), 31.13 (s), 29.35 (s), 28.44 (s), 28.30 (s), 25.46 (s), 22.02 (s), 13.89 (s).

^{19}F NMR (376 MHz, DMSO- d_6): δ (ppm)= -78.71 (s).

2.4.9. Synthesis of 1-hexyl-3-methylimidazolium bis(trifluoromethylsulfonyl)imide [C_6C_1im][NTf_2]



Scheme 12. Synthesis of [C_6C_1im][NTf_2]

Using the procedure described in Weber et al.⁴¹ 1-Hexyl-3-methylimidazolium chloride (15.13 g, 0.0746 moles) and, lithium bis(trifluoromethylsulfonyl)imide (17.66 g, 0.0784 moles, 1.05 eq) dissolved in 100 mL of deionized water individually and then 150 mL of DCM added to the mixture. DCM layer was washed with deionized water (4×100 mL) until the absence of halide was confirmed with 0.1M AgNO₃ solution. The DCM was removed by rotary evaporator and the IL formed was dried on high vacuum at 55°C to yield [C₆C₁im][NTf₂] as a pale-yellow liquid.

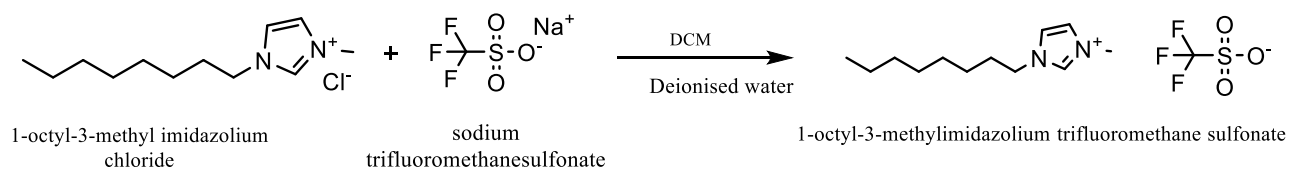
Yield: 25.4 g, 0.0506 mol, 76%

¹H NMR (400 MHz, DMSO-d₆): δ(ppm)= 9.11 (s, 1H), 7.77 (t, *J* = 1.8 Hz, 1H), 7.70 (t, *J* = 1.7 Hz, 1H), 4.16 (t, *J* = 7.2 Hz, 2H), 3.86 (s, 3H), 1.85 – 1.73 (m, 2H), 1.36 – 1.19 (m, 6H), 0.94 – 0.84 (m, 3H).

¹³C {¹H} NMR (101 MHz, DMSO-d₆): δ(ppm)= 136.47 (s), 123.60 (s), 122.24 (s), 119.47 (q, *J* = 323 Hz), 48.76 (s), 35.71 (s), 30.51 (s), 29.30 (s), 25.11 (s), 21.83 (s), 13.77 (s).

¹⁹F NMR (376 MHz, DMSO-d₆): δ(ppm)= -78.72 (s).

2.4.10. Synthesis of 1-octyl-3-methylimidazolium trifluoromethanesulfonate [C₈C₁im][OTf]



Scheme 13. Synthesis of [C₈C₁im][OTf]

Using the procedure described in Brooks et al.⁴² Sodium trifluoromethanesulfonate (40.91 g, 0.2378 mol, 1.09 equiv.) was added to 1-octyl-3-methylimidazolium chloride (50.37 g, 0.2182 mol) dissolved in DCM (150 mL). The slurry formed was stirred for 72 hours then filtered. The resultant filtrate was washed repeatedly with water (5×10 mL) until no halide detected with 0.1M silver nitrate solution. The solvent was removed, and resultant liquid dried in vacuo at 60°C to yield [C₁₀C₁im][OTf] as a clear colorless liquid.

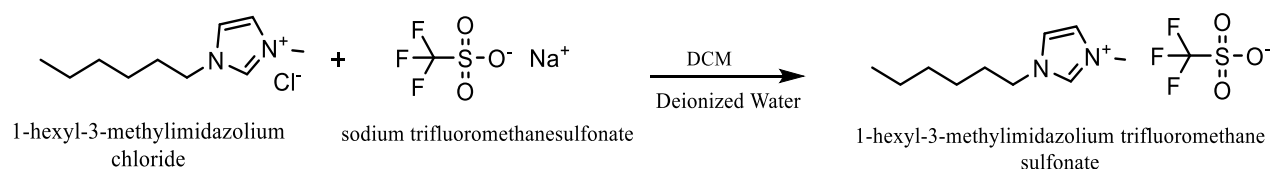
Yield: (57.9 g, 0.1675 mol, 76%).

¹H NMR (400 MHz, DMSO-d₆): δ(ppm)= 9.10 (s, 1H), 7.77 (t, *J* = 1.8 Hz, 1H), 7.71 (t, *J* = 1.7 Hz, 1H), 4.16 (t, *J* = 7.2 Hz, 2H), 3.86 (s, 3H), 1.86 – 1.73 (m, 2H), 1.28 (m, 10H), 0.87 (t, *J* = 6.9 Hz, 3H).

^{13}C { ^1H } NMR (101 MHz, DMSO- d_6): $\delta(\text{ppm})= 136.47$ (s), 123.59 (s), 122.25 (s), 48.77 (s), 35.72 (s), 31.13 (s), 29.35 (s), 28.44 (s), 28.30 (s), 25.47 (s), 22.02 (s), 13.90 (s).

^{19}F NMR (376 MHz, DMSO- d_6): $\delta(\text{ppm})= -77.76$ (s).

2.4.11. Synthesis of 1-hexyl-3-methylimidazoliumtrifluoromethanesulfonate [C₆C₁im][OTf]



Scheme 14. Synthesis of [C₆C₁im][OTf]

Using the procedure described in Brooks et al.⁴² 1-Hexyl-3-methylimidazolium chloride (43.53 g, 0.2147 mol) was dissolved in DCM (150 mL). Sodium trifluoromethanesulfonate (40.26 g, 0.2340 mol, 1.09 equiv.) was added and the slurry formed was stirred for 72 hours. The resultant slurry was filtered and the filtrate successively washed with water (4×10 mL) until no halide was detected with concentrated silver nitrate solution. The solvent was removed by rotary evaporation and the resultant liquid dried in vacuo at 60°C to yield [C₆C₁im][OTf] as a clear colorless liquid.

Yield: 50.4 g, 0.1592 mol, 74%

^1H NMR (400 MHz, DMSO- d_6): $\delta(\text{ppm})= 9.09$ (s, 1H), 7.76 (t, $J = 1.8$ Hz, 1H), 7.69 (t, $J = 1.7$ Hz, 1H), 4.15 (t, $J = 7.2$ Hz, 2H), 3.85 (s, 3H), 1.84 – 1.72 (m, 2H), 1.34 – 1.18 (m, 6H), 0.90 – 0.81 (m, 3H).

^{13}C { ^1H } NMR (101 MHz, DMSO- d_6): $\delta(\text{ppm})= 136.46$ (s), 123.60 (s), 122.24 (s), 48.76 (s), 35.72 (s), 30.51 (s), 29.30 (s), 25.11 (s), 21.84 (s), 13.79 (s).

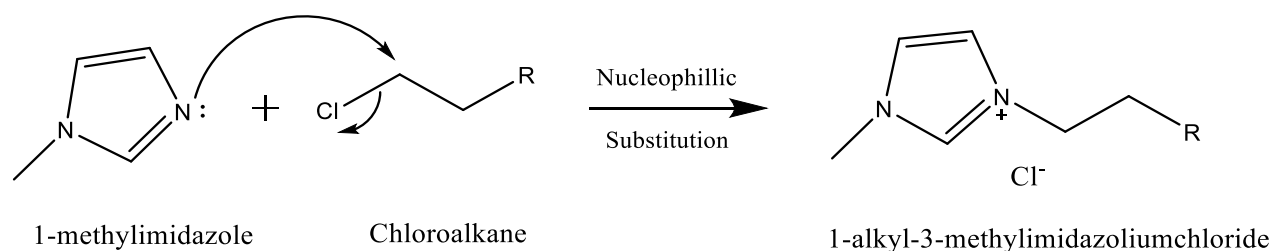
^{19}F NMR (376 MHz, DMSO- d_6): $\delta(\text{ppm})= -77.77$ (s).

CHAPTER 3: RESULTS AND DISCUSSION

3.1. Synthesis of Ionic Liquids

3.1.1. Synthesis of Imidazolium Halides Ionic Liquids

The reaction of amines with alkyl halides to form quaternary ammonium salts was originally studied by the Menshutkin.⁴⁴ These reactions involve amine nucleophile with the halide leaving group. This results in the corresponding ammonium halide salt. The synthesis of imidazolium chloride ILs was based on these Menshutkin reactions, with the general procedure depicted in **Scheme 15**.⁴⁵ [C₁₀C₁im]Cl, [C₈C₁im]Cl and [C₆C₁im]Cl were prepared in this way with their specific syntheses depicted in **Schemes 4, 9 and 10**. The alkyl halide is used in a slight excess as it is the easier component to remove during the subsequent purification steps.

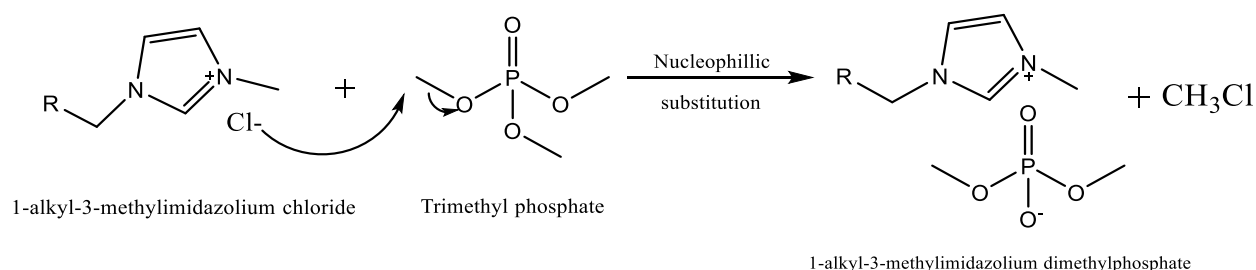


Scheme 15. General mechanism for the formation of 1-alkyl-3-methylimidazolium chlorides.

The reaction conditions for the three ILs [C₁₀C₁im]Cl, [C₈C₁im]Cl and [C₆C₁im]Cl were similar although the time taken varied significantly with [C₆C₁im]Cl taking 24 days to reach a reasonable level of conversion whereas [C₁₀C₁im]Cl took 40 days. The difference in time was most likely due to subtle differences in experimental setup between reactions leading to slightly different actual reaction temperatures being obtained each time, for example the depth of the thermostat in the oil bath. The purification of these ILs involved washing with large volumes of diethyl ether to remove remaining 1-methylimidazole. The effectiveness of washing was reduced due to the viscosity of these ILs and their miscibility with more polar solvents such as ethyl acetate. [C₁₀C₁im]Cl and [C₈C₁im]Cl were synthesized in good yields with [C₆C₁im]Cl prepared in very good yield.

3.1.2. Synthesis of Imidazolium Dimethyl phosphate Ionic Liquids

The first reported use of dimethylphosphates as an IL ion was by Wasserscheid and coworkers in 2007.⁴⁶ The original method for the synthesis of imidazolium dimethylphosphate ILs involved the direct nucleophilic attack of 1-alkylimidazole on trimethylphosphate. This method is limited by the availability of the appropriate 1-alkylimidazole precursor. A more recently established method is the general approach shown in **Scheme 16** which was used for the synthesis of [C₁₀C₁im][Me₂PO₄] as shown in **Scheme 8**.⁴⁷ This follows a nucleophilic substitution mechanism where the Cl⁻ ion attacks the methyl group of trimethyl phosphate forming methyl chloride with dimethyl phosphate as the leaving group. Trimethylphosphate is used in a slight excess to ensure the complete removal of halide.



Scheme 16. General mechanism for the formation of 1-alkyl-3-methylimidazolium dimethyl phosphate.

[C₁₀C₁im][Me₂PO₄] was formed in fair yield. This was likely due to the loss of the IL during the washing phase as initial attempts to wash out residual trimethyl phosphate using diethyl ether led to the formation of a single phase due to the miscibility of the IL in the diethyl ether. Subsequent washings were done with hexane which leads to two separate phases and the complete removal of TMP from the product.

3.1.3. Synthesis of Imidazolium Trifluoromethanesulfonate Ionic Liquids

ILs with the trifluoromethanesulfonate ([OTf]⁻) anion were synthesized by the metathesis reaction of halides (Cl⁻, Br⁻) with sodium trifluoromethanesulfonate (NaOTf).⁴⁸ This procedure relies on the relatively greater solubility of NaOTf compared to NaCl or NaBr in dichloromethane and the preferred partitioning of [C_xC₁im][OTf] in dichloromethane compared to water. Hence, the method involves stirring a slurry of [C_xC₁im]Cl and a slight excess of NaOTf in dichloromethane for 72 hours before filtration and then washing the dichloromethane with deionized water until all residual halide is removed.

The specific synthesis of [C₁₀C_{1im}][OTf], [C₈C_{1im}][OTf] and [C₆C_{1im}][OTf] are shown in **Schemes 7, 13 and, 14**. This resulted in very good yield of [C₁₀C_{1im}][OTf] and good amounts of both [C₈C_{1im}][OTf] and [C₆C_{1im}][OTf] formed.

3.1.4. Synthesis of Imidazolium bis(trifluoromethylsulfonyl)imide ILs

The synthesis of [NTf₂]⁻ ILs also occurred through a salt metathesis reaction in which the halide anion was replaced by [NTf₂]⁻. The ILs obtained by this process are hydrophobic and insoluble in water.⁴⁹ This method depends on the greater comparative solubility of LiNTf₂ in dichloromethane relative to LiCl. The relatively greater solubility of LiCl in water allows the halides to more easily be washed out. The ILs [C₁₀C_{1im}][NTf₂], [C₈C_{1im}][NTf₂] and, [C₆C_{1im}][NTf₂] were prepared by this method as shown from **Schemes 6, 11 and 12**. The excess of chloride was removed by repeated washings with water. [C₁₀C_{1im}][NTf₂] and [C₈C_{1im}][NTf₂] was obtained in excellent yield, and good yield obtained for [C₆C_{1im}][NTf₂].

3.2. Set up of Model Reactions

3.2.1. Dehydration of Alcohol as a Model Reaction

The dehydration of alcohols was selected as a model reaction to study for a variety of factors. Firstly, the reaction does not undergo a significant change in charge development along the reaction coordinate which avoids the reorganization of the solvent around the transition state and allows the effect of solvent structure to be more clearly established. Secondly, these reactions have been widely studied and so the reaction mechanism is well understood allowing solvent effects to be more clearly identified. Thirdly, these reactions can act as simple models for the decomposition of sugars obtained from biomass which is of growing importance particularly within IL solvents.

The use of strong acids such as HCl, H₂SO₄ to increase the rate of alcohol dehydration reactions has been known from many years. Some methods have been developed in recent years to enable these dehydrations to occur in the absence of a strong acid catalyst, including the use of superheated water, micelles and neoteric solvents such as ILs.⁵⁰ For the simplicity of the reaction system, here we have aimed to explore the use of ILs in the absence of added strong acids to avoid confounding factors arising from the basicity of the IL anion. The design of effective solvents for alcohol dehydration processes in the absence of corrosive strong acid catalysts

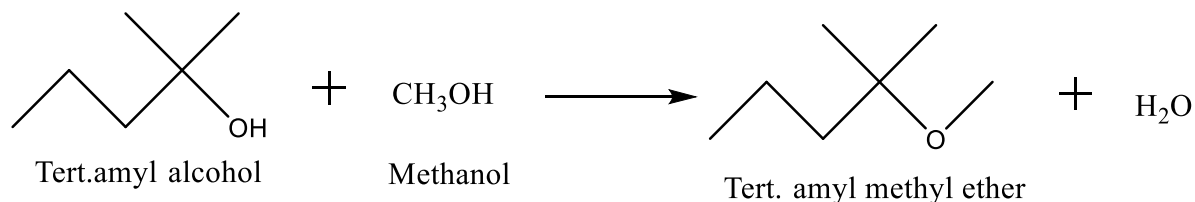
would be significant for green chemistry if it did not lead to a correspondingly large increase in energy input.

The first step in understanding the effect of IL solvents on the dehydration of alcohols is establishing a model system. Key requirements of this system are that it is able to be easily monitored within a reasonable timeframe and it produces a relatively simple product distribution. For simplicity this means ideally the formation of non-volatile products so that solution phase extraction and analysis procedures can be employed.

The reactivity of primary and secondary alcohols in [C₁₀C₁im][NTf₂] was initially explored. These alcohols with high boiling points help to observe the dehydration reaction without affecting the product formation from harsh reaction conditions. To see the effect of ILs including long chains with more hydrophobic anions [C₁₀C₁im][NTf₂] was selected first.

3.2.2. Tert. Amyl Alcohol and Methanol

The first model reaction of alcohols explored, in this project was the nucleophilic substitution of tert-amyl alcohol and methanol analysed to produce the corresponding tert-amyl methyl ether.



Scheme 17. General reaction for the formation of tert. amyl methyl ether.

The 1,1-methylethylene and trimethylethylene in the ratio of (1:7) was reported from the dehydration of tert. amyl alcohol refluxed with 15% of sulphuric acid.⁵¹ Whereas, the formation of tert. amylmethyl ether in almost same amount with highest yield of butyl methyl ether reported from the reaction between tert. butyl alcohol and methanol at 200°C.⁵²

This reaction was explored by heating the reaction mixture to 70°C for 192 hours although no product formation could be observed by NMR. Even increasing the temperature to 120 °C for 24 hours did not yield any evidence of product formation **reaction 1 and 2, Table 2**. Due to this and the potential to form volatile by-products that would be unable to be quantified it was decided not to continue further with this model reaction.

Table 2. Results of reactions between tert-amyl alcohol and methanol in [C10C1im][NTf2]. Reactants and IL were prepared in a volume ratio of tert-amyl alcohol: methanol: IL of 1:2:3.

Rxn. No.	Mole Fraction Tert-amyl alcohol+ methanol	Reaction Conditions	NMR Results
1	0.147 +0.737	70°C, 192 hours glass vial	No clear product formation from NMR
2.	0.147 +0.737	120°C, 24 hours , Hydrothermal Reactor	No clear product formation from NMR

3.2.3. 1,4-Cyclohexandiol

The effect of [C₁₀C₁im][NTf₂] on the dehydration of 1,4-cyclohexandiol was examined at 150°C for 24 hours. ¹H NMR showed the possibility of alkene formation due to the presence of additional signals at 5.5 ppm.

The quantification of reaction progression for 1,4-cyclohexandiol was complicated by the difficulty in separating the reactant from the IL to enable quantification by GC-FID methods. Attempts to use a silica column with DCM as an eluent were unsuccessful due to the poor solubility of 1,4-cyclohexandiol in this solvent. Attempts to use solvent extraction were similarly unsuccessful. Given these difficulties it was decided that this represents an unsuitable model system for further study.

3.2.4. Octan-1-ol

Octan-1-ol was selected because of its high boiling point and simple structure and the expected product (oct-1-ene) is not volatile. Whereas, in the case of shorter chained alcohols such as ethanol and butanol their low boiling points and the markedly lower boiling points of the expected alkene products would limit the ease of reaction monitoring given the products would form as gases.

In the case of octan-1-ol after 72 hours at 120°C the reaction mixture did not display any evidence of product formation by NMR. The reaction mixture was transferred from a glass vial

to a hydrothermal reactor to allow the reaction to continue at 180°C for 120 hours. The reaction mixture was shifted to the reactors to avoid the evaporation of any volatile products formed during the reaction and due to safety concerns. Moreover, no significant product formation was observed for the octan-1-ol reaction in $[C_{10}C_{iim}][NTf_2]$ after 120 hours at 180°C. The NMR results shown in **Figure 10** demonstrate small peak area 5.5 ppm which is inductive of alkenes, however this was only present in trace amounts after 120 hours.

Given the absence of a notable reaction even under these elevated temperatures for prolonged reaction times, it was decided to examine more reactivity of secondary rather than primary alcohols as potential model reaction substrates.

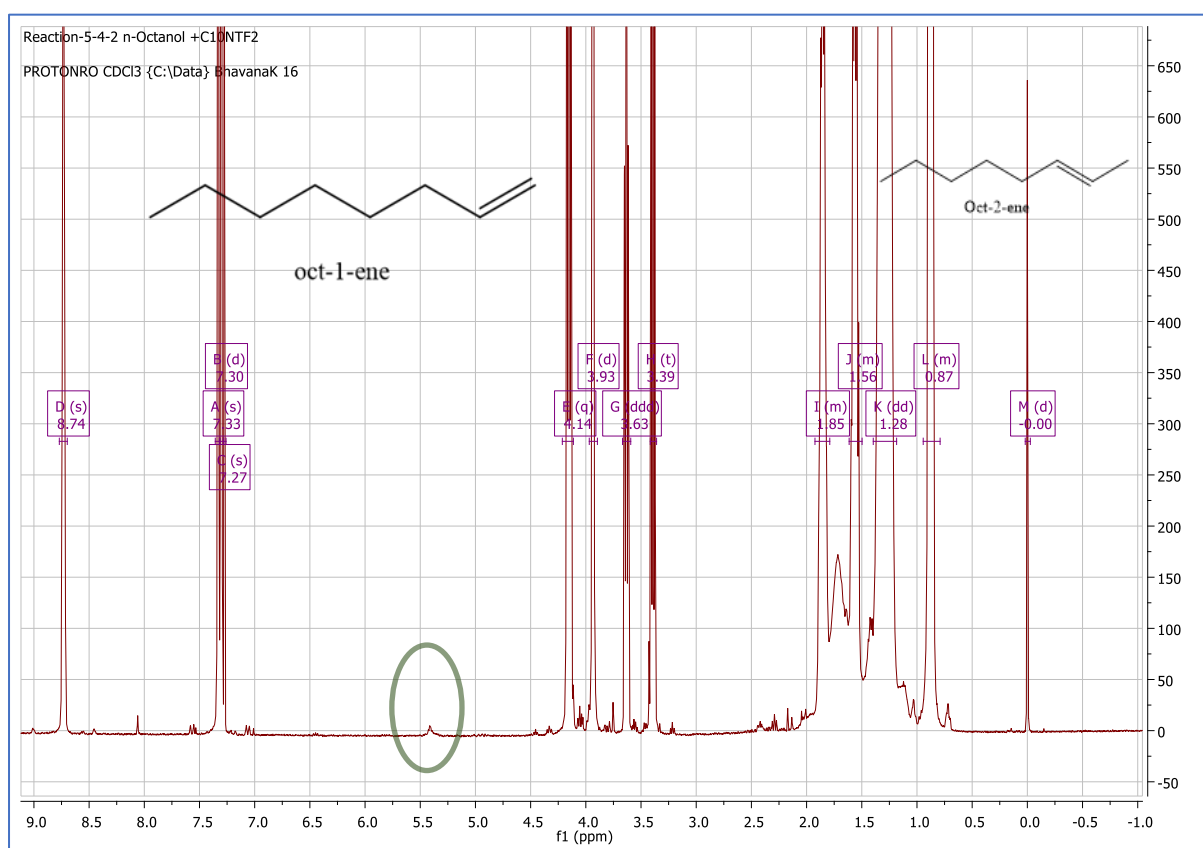
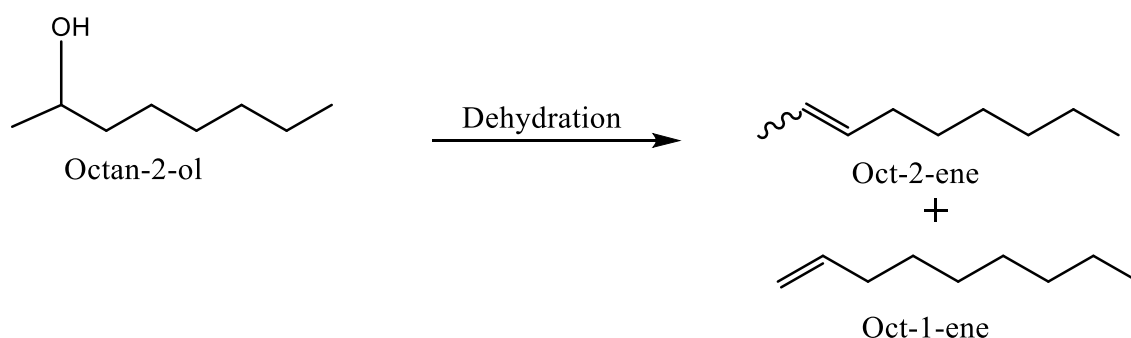


Figure 10. 1H NMR after 120 hours for the reaction of octan-1-ol in $[C_{10}C_{iim}][NTf_2]$.

3.2.5. Octan-2-ol

Octan-2-ol was selected as a substrate to explore the reactivity of secondary alcohols seeing as octan-1-ol didn't react under the chosen conditions. The reaction of octan-2-ol in $[C_{10}C_{iim}][NTf_2]$ after 120 hours at 120°C in glass vial shown the evidence of product formation. The reaction was again monitored at 180°C for 24 hours in hydrothermal reactor to

confirm the product formation as shown in **Table 3**. The results from $^1\text{H NMR}$ in **Figure 11** show the presence of several peaks between 5 to 6 ppm which provides evidences for alkene formation. Hence, it was of interest to explore the rate of formation of the alkene product.



Scheme 18. General reaction for dehydration of octan-2-ol.

Table 3. Results of initial reactions of octan-2-ol in $[\text{C}_{10}\text{C}_{1}\text{im}][\text{NTf}_2]$

Rxn. No.	(Reactant: Solvent Ratio) (Vol.: Vol.)	Mole Fraction Alcohol	Reaction Conditions	NMR Results
3.	1:1	0.715	120°C, 120 hours, Glass Vial	Evidence for alkene formation.
4.	1:5	0.712	180°C, 24 hours, hydrothermal reactor	Evidence for alkene formation.

Using the reaction conditions from **Reaction 4, Table 3**, specifically a 1:5 volume ratio of octan-2-ol: $[\text{C}_{10}\text{C}_{1}\text{im}][\text{NTf}_2]$ heated at 180°C, the reaction was monitored after 1, 2,3,4 and 24 hours.

Table 4. Relative integrals of the alkene peak at 5.4 ppm versus the octan-2-ol peak at 3.8 ppm

Sr. No.	Time	Relative Integral
1	1 hour	0.19
2	2 hour	0.18
3	3 hour	0.43
4	4 hour	0.42

The similarity in results as shown in **Table 4** was most likely due to the requirement that the reactor was cooled after each interval to draw the sample for NMR. This interrupted the maintenance of temperature at each interval and the lag for the internal temperature to increase back to 180 °C could not be accurately accounted for. Hence, **reaction 4** was repeated and monitored after 4 and 24 hours to avoid issues associated with repeated monitoring. The maximum alkene formation after 24 hours with no evidences of alcohol was confirmed from ¹H NMR.

These results highlighted that the dehydration of octan-2-ol is a plausible model reaction although the formation of isomeric products, as shown in **Figure 11**, does complicate the product analysis.

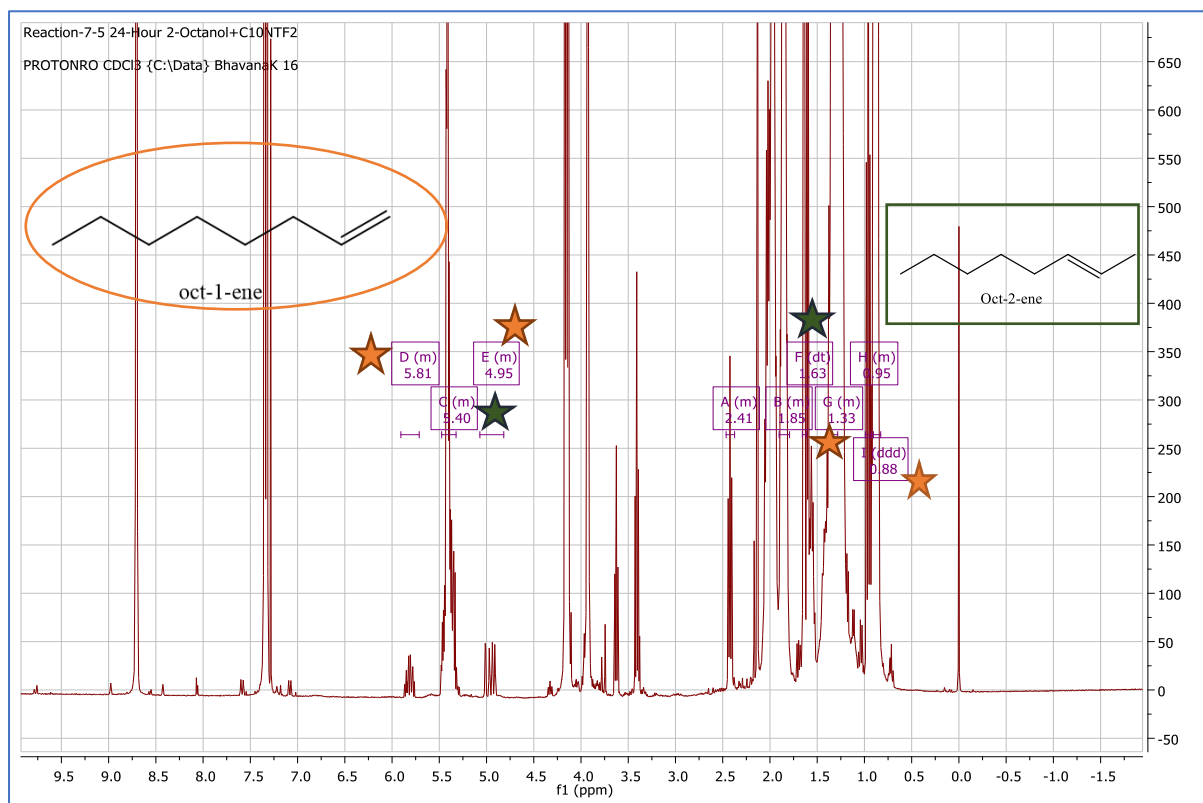


Figure 11. ^1H NMR after 24hours for reaction of octan-2-ol in $[\text{C}_{10}\text{C}_{11}\text{im}][\text{NTf}_2]$ at 180°C .

★ Oct-1-ene peaks; ★ Oct-2-ene peaks

3.2.6. Cyclohexanol

The formation of alkenes was obtained with octan-2-ol so, we explored the effect of $[\text{C}_{10}\text{C}_{11}\text{im}][\text{NTf}_2]$ on the dehydration of cyclohexanol shown in **Table 5** to determine the generality of secondary alcohol dehydration. Cyclohexanol would also yield a simpler distribution of products due to the lack of possible isomerism. No product formation was obtained at 120°C after 2 or 4 hours. So, the temperature was raised to 150°C and product formation was identified by ^1H NMR after 4 hours. To analyse whether improved product formation could be observed the reaction was monitored at 180°C for two hours. A noticeable amount of product formation was seen confirmed from ^1H NMR as shown in **Figure 12**.

Table 5. Cyclohexanol dehydration in [C10C1im][NTf2] under different reaction conditions.

Rxn. No.	(Cyclohexanol: [C ₁₀ C ₁ im][NTf ₂]) (Vol.: Vol.)	Mole Fraction Alcohol	Reaction Conditions	NMR Results
5.	1:5	0.654	120°C, 4hours	No product formation after 2 or 4 hours.
6.			150°C, 4hours	Evidence of product formation after 4 hours.
7.			180°C, 2hours	Apparent conversion of reactants after 2 hours.

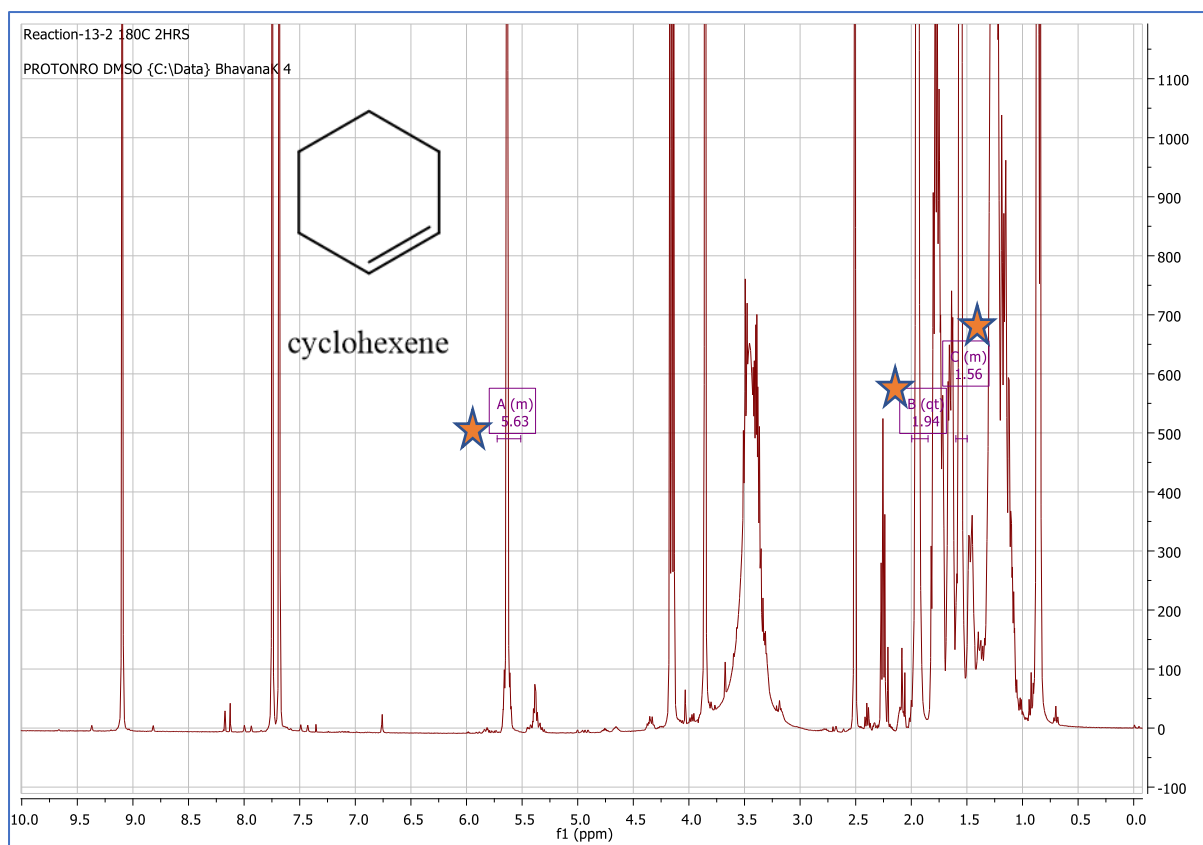


Figure 12. ^1H NMR showing the formation of cyclohexene from cyclohexanol after two hours at 180°C in $[\text{C}_{10}\text{C}_{11}\text{m}] [\text{NTf}_2]$.

★ Cyclohexene peaks

3.3. Analytical Protocol

While NMR was able to be used to detect the existence of products, as has been discussed above, it was not possible to use NMR for the full quantification of reactants and products in the reaction mixture due to peak overlap with the IL and other compounds in the solution. To enable the full quantification of the reaction mixture, gas chromatography (GC) was explored due to the ease of separation and quantification of reaction products.

3.3.1. Selection of Internal Standard

To establish a GC-FID method, a suitable internal standard for the quantification of products was required. A key requirement for an internal standard is that it is stable under the reaction conditions. Mesitylene was identified as a possible internal standard and added to octan-2-ol and IL under the same reaction conditions as shown in **Table 6**.

Table 6. Dehydration reaction to check the reactivity of mesitylene with octan-2-ol in presence of $[C_{10}C_{1im}][NTf_2]$

Rxn. No.	Mesitylene: 2-Octanol: $[C_{10}C_{1im}][NTf_2]$ (Mass)	Alcohol	Reaction Conditions	NMR Results
8.	1: 5: 20	0.684	180°C, 24 hours.	No evidence of mesitylene reaction

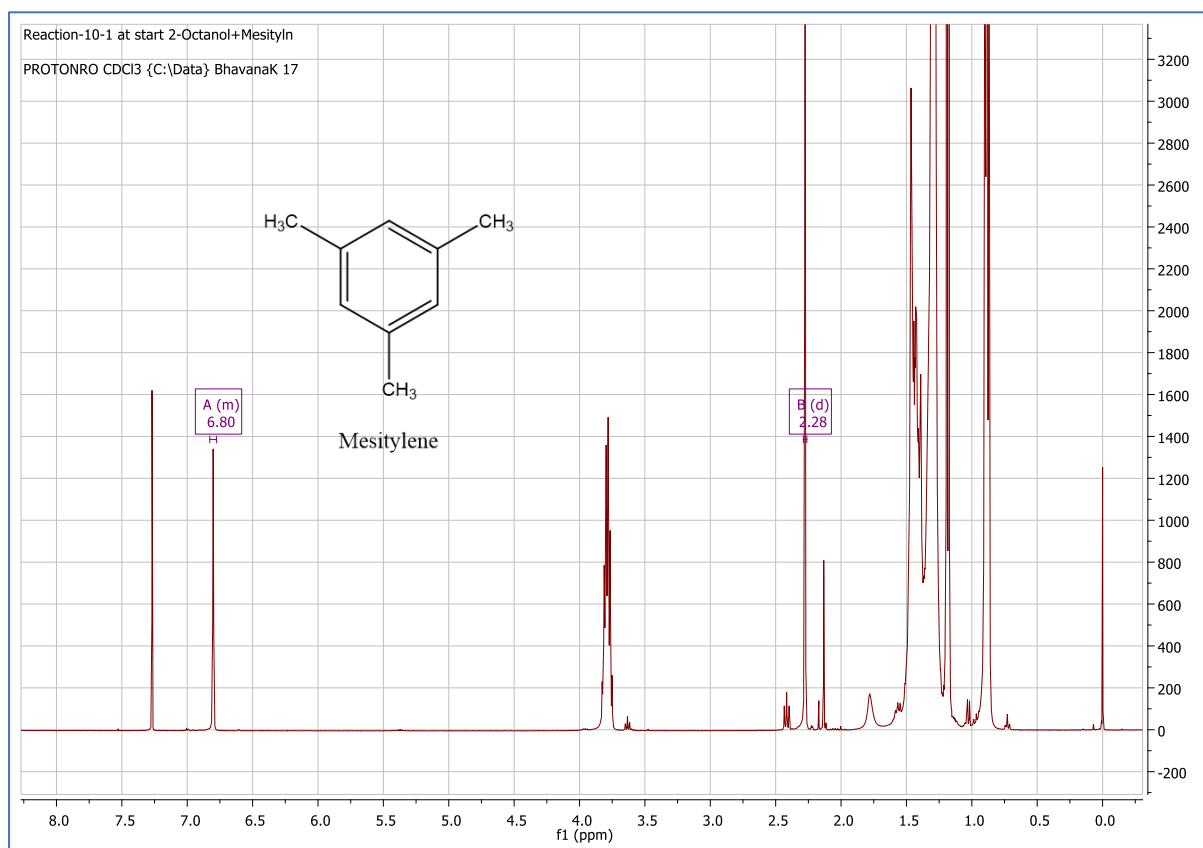


Figure 13. 1H NMR before reaction of octan-2-ol and $[C_{10}C_{1im}][NTf_2]$ exploring the stability of mesitylene as an internal standard.

A sample was taken before the reaction which shows the presence of mesitylene peaks seen by 1H NMR in **Figure 13**. A sample taken after the reaction indicated that mesitylene remained intact in the reaction mixture and didn't react under the given reaction conditions as shown in **Figure 14**. In particular there were no additional aromatic peaks that could be identified not any changes to the methyl protons. The integral of mesitylene with respect to

IL was 2.99 before reaction and 2.98 after reaction demonstrating that it did not change under the reaction conditions.

Unexpectedly, no alkene formation was revealed from ^1H NMR after 24 hours reaction as compared to the observations from **Reaction 4, table 3**. During the reaction there was half an hour power cut that made the reaction slower. The sample was taken 30mins later after 24hours to compensate but the power cut may have had a more pronounced effect on the reactor temperature.

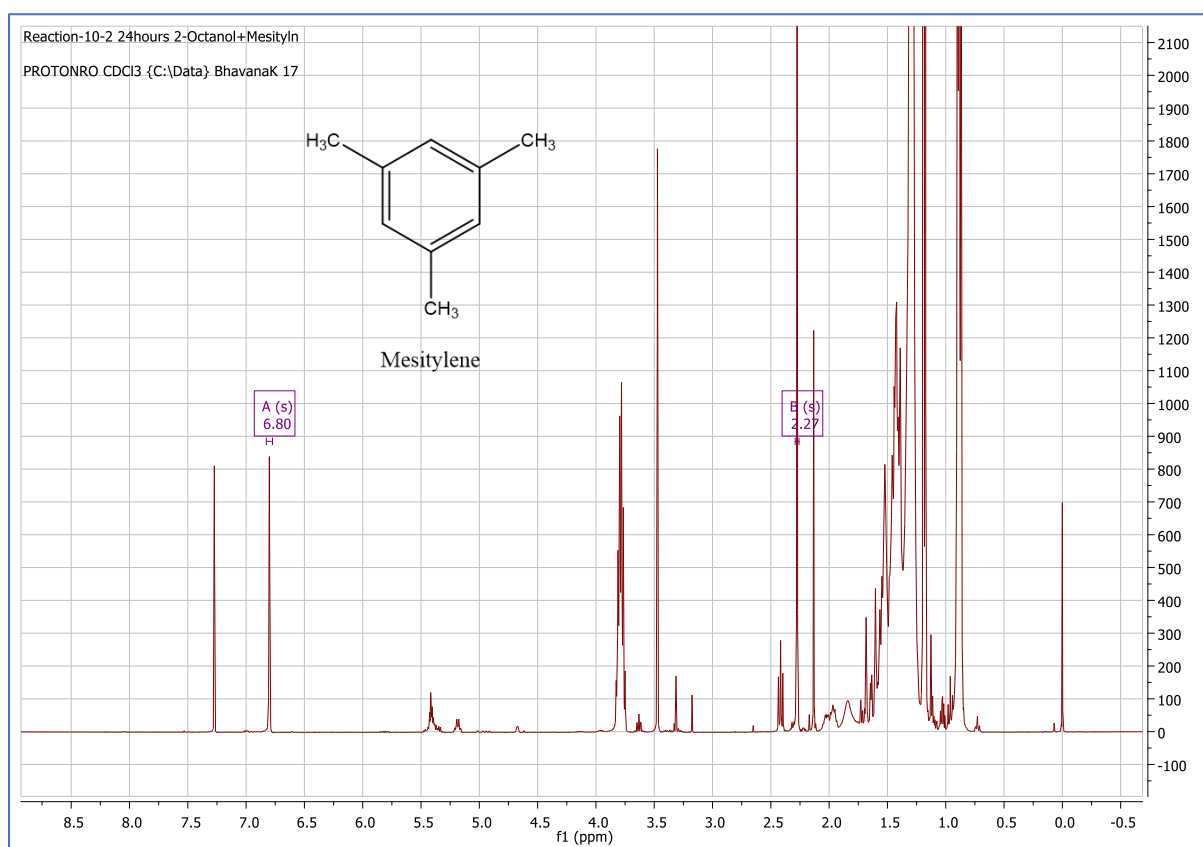


Figure 14. ^1H NMR after 24hours of reaction between octan-2-ol and $[\text{C}_{10}\text{C}_{1\text{im}}][\text{NTf}_2]$ with mesitylene as an internal standard.

As the mesitylene was found to be unreacted under these reaction conditions so, it is potentially suitable for use as a standard. Whereas, to separate the reactants/products and standard on GC-FID a set of extraction conditions needed to be developed.

3.4. Establishing the GC-FID Method analysis

Octan-2-ol and cyclohexanol both appeared to give promising dehydration results, the ability to separate, identify and quantify the reactants and the products formed from these reactions was explored.

3.4.1. Cyclohexanol Calibration

The GC-FID chromatograms for cyclohexanol products and standards was shown in **Figure 15 and 16** respectively. Dicyclohexyl ether present in **Figure 15** was confirmed by GC-MS. as an authentic standard of this compound was not available.

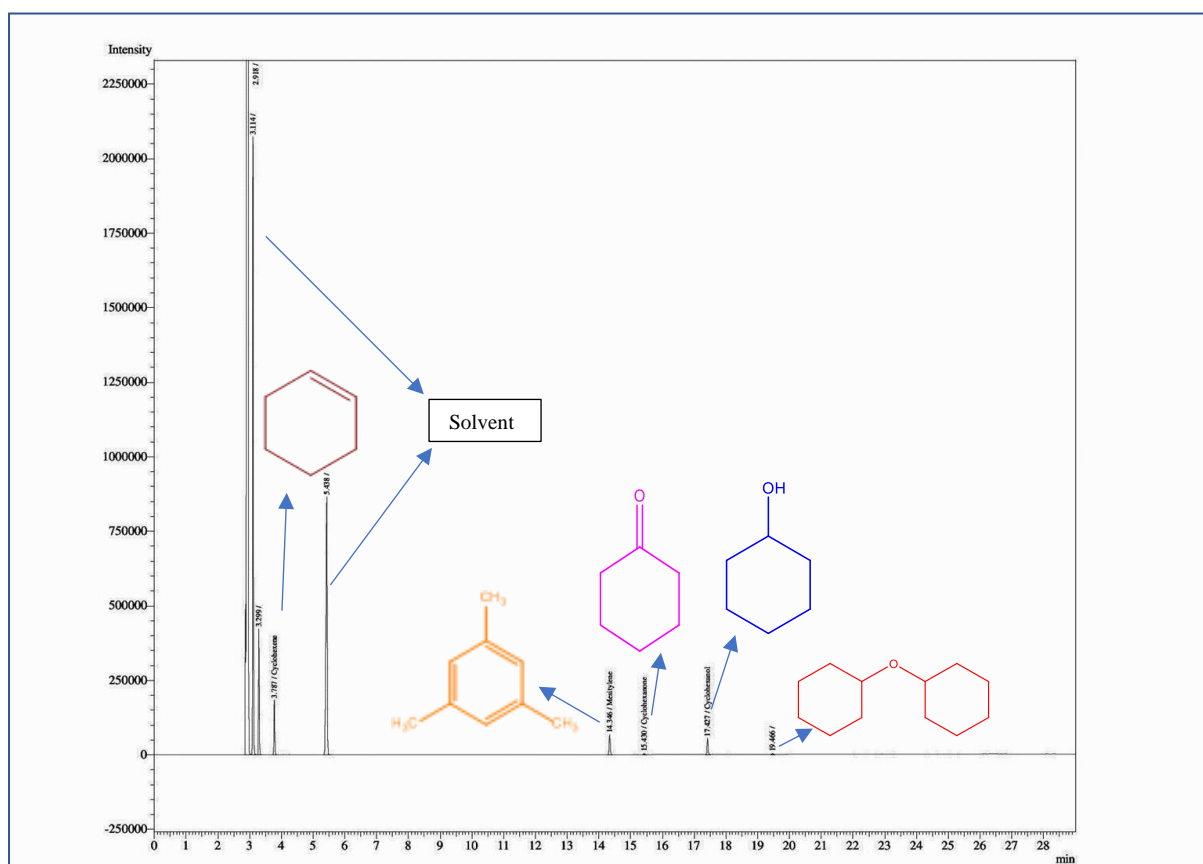


Figure 15. GC-FID chromatogram of a cyclohexanol reaction mixture with major products assigned.

The calibration of cyclohexanol and major products was performed using the GC method described above. Standards for cyclohexanol, cyclohexanone and cyclohexene were prepared along with the mesitylene internal standard. Dicyclohexyl ether was not calibrated as we did not have access to an appropriate standard and it was only present in trace amounts. Five vials

with different mass ratios of the four standards in each vial were prepared as shown in **Table 7**. Linear calibration curves with excellent fits were obtained from those mass ratios for each of the standards used as shown in **Figures 17-19**.

Intensity

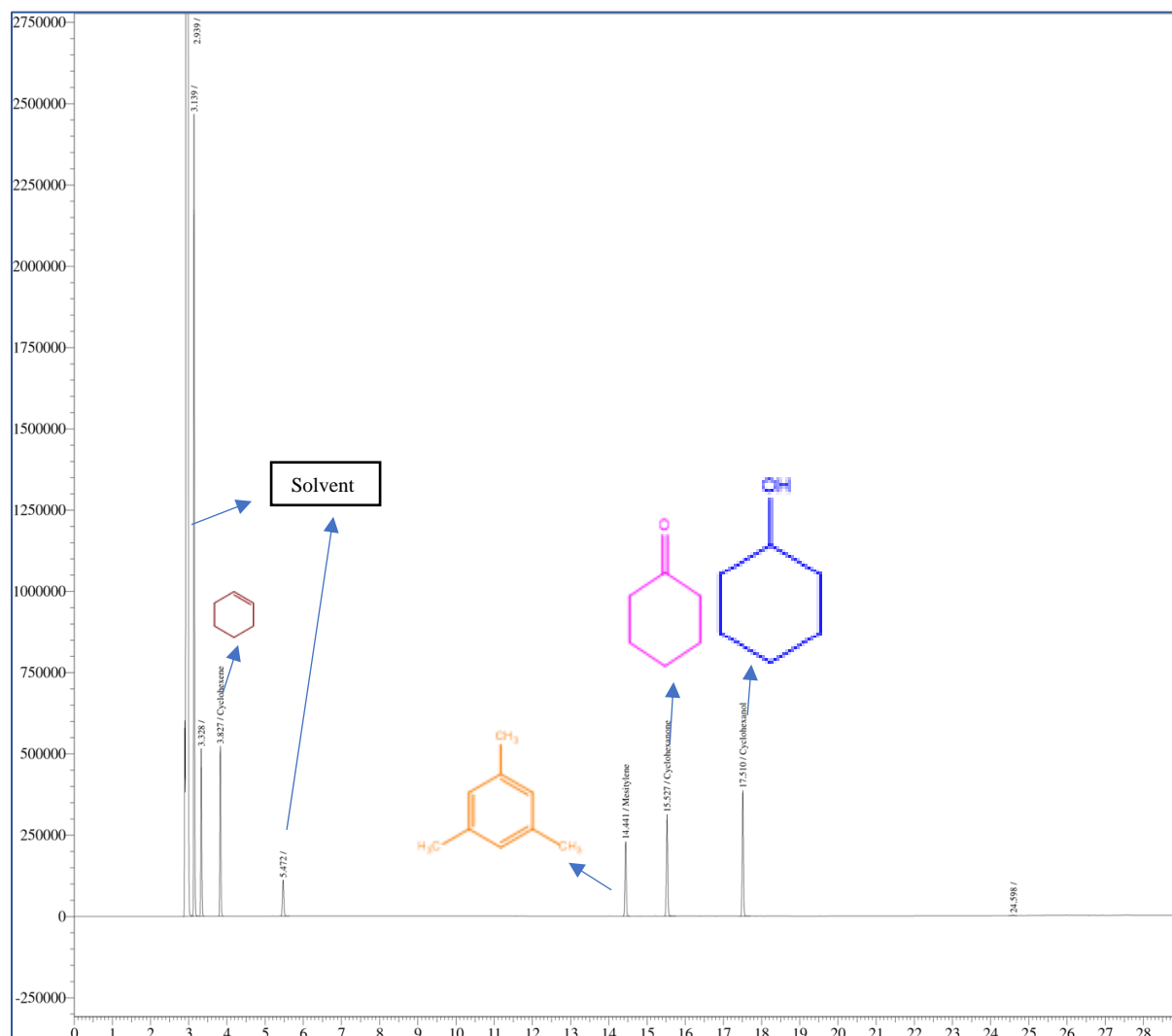


Figure 16. GC-FID chromatogram of cyclohexanol standards.

Table 7. Mass ratio of cyclohexanol calibration standards used for GC-FID analysis

Ratio	Mesitylene	:	Cyclohexanol	:	Cyclohexene	:	Cyclohexanone
Vial 1	1	:	5	:	5	:	5
Vial 2	1	:	2	:	2	:	2
Vial 3	1	:	1	:	1	:	1

Ratio	Mesitylene	Cyclohexanol	Cyclohexene	Cyclohexanone
Vial 4	2	1	1	1
Vial 5	5	1	1	1

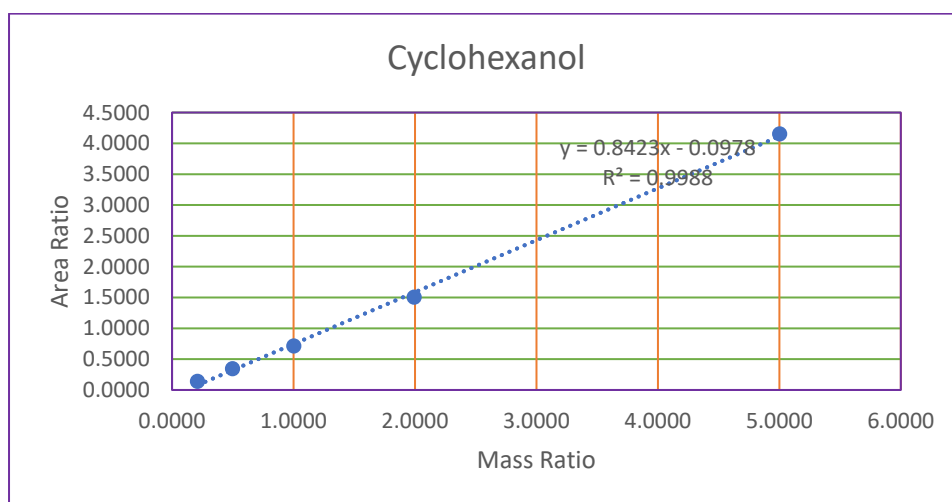


Figure 17. GC-FID calibration curve for cyclohexanol.

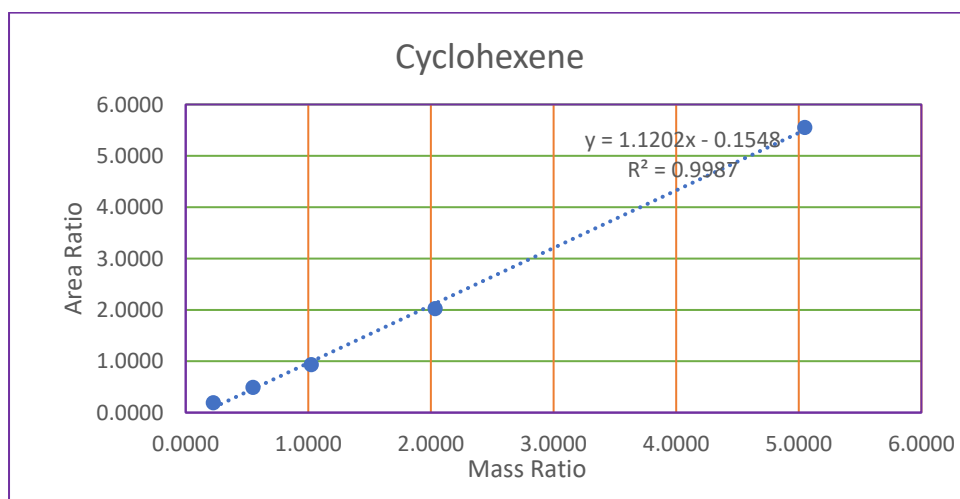


Figure 18. GC-FID calibration curve for cyclohexene.

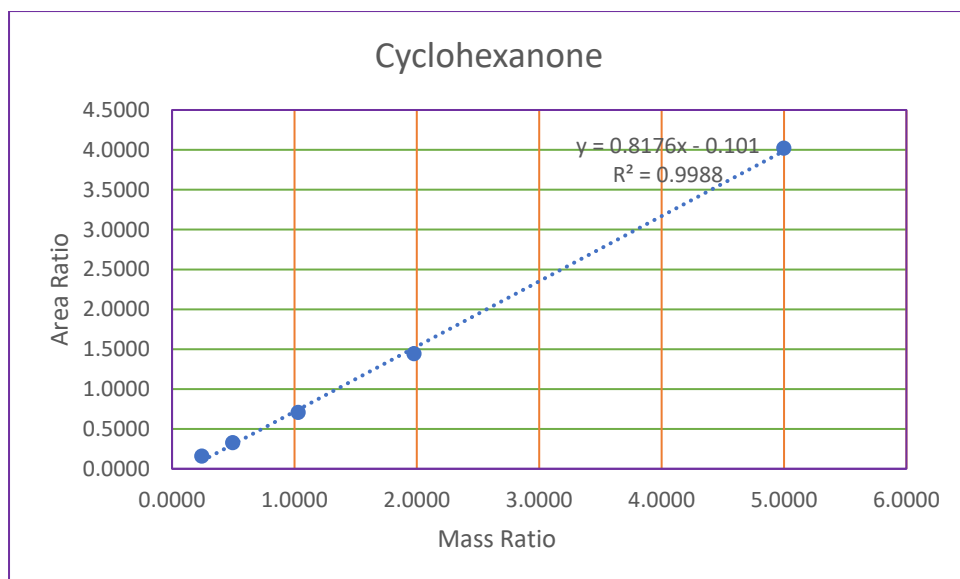


Figure 19. GC-FID calibration curve for cyclohexanone.

3.4.2. Cyclohexanol Calibration 2

As the extraction method was developed, an unexpected change to the GC-FID parameters occurred. As the GC-FID is shared instrument so this is possibly inference by the other user. After restoring the initial parameters, the calibration with cyclohexanol was repeated using the same mass as in **Table 7**. These calibration curves are depicted in **Figures 20-22**.

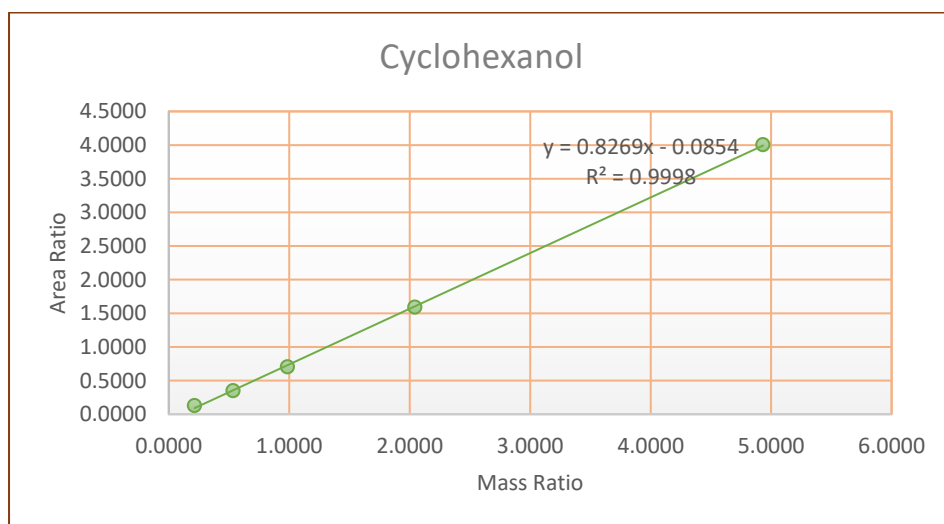


Figure 20. Cyclohexanol GC-FID calibration curve.

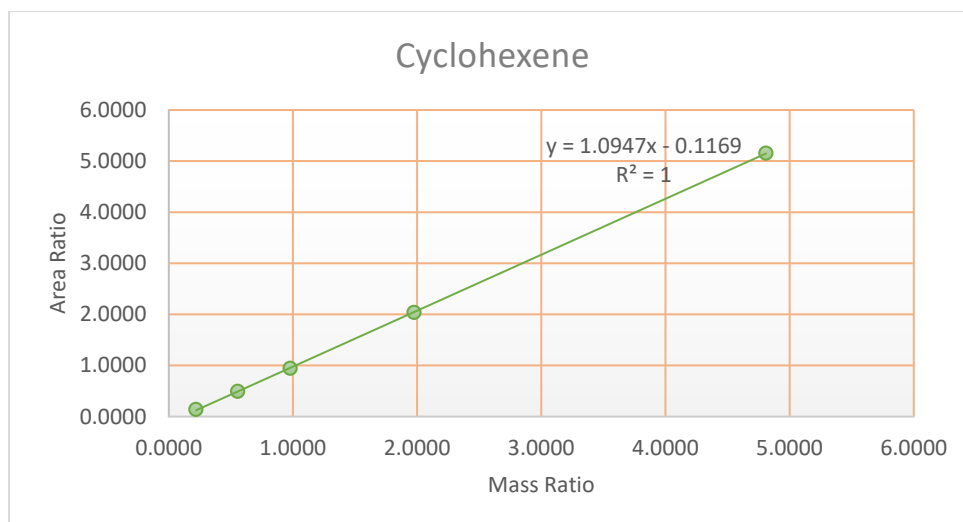


Figure 21. Cyclohexene GC-FID calibration curve.

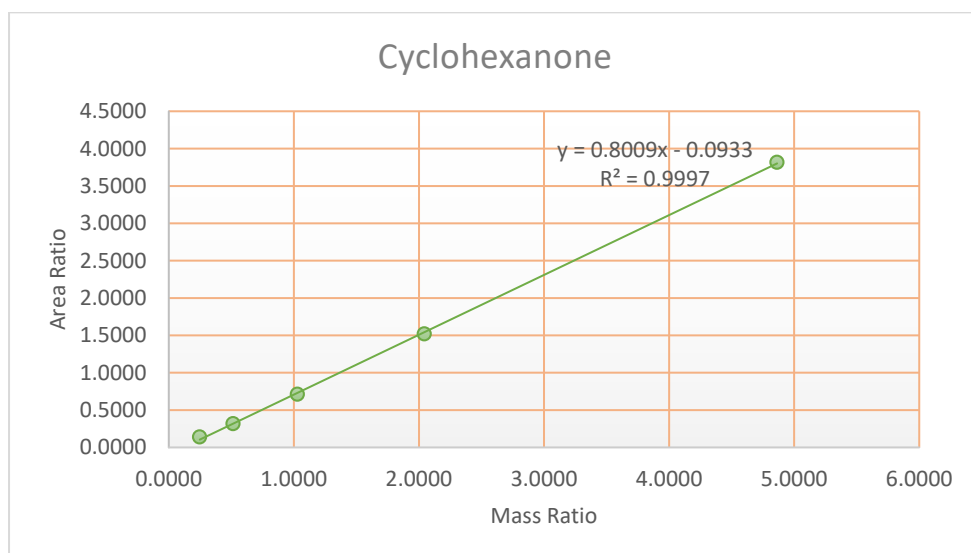


Figure 22. Cyclohexanone GC-FID calibration curve.

3.4.3. Octan-2-ol GC-FID Method

A GC-FID method to separate, identify and quantify the products of the octan-2-ol reactions was also established (**Figures 23 and 24**). Many of the other isomers of alkene such as oct-4-ene, oct-3-ene also identified using GC-MS, however were present in trace amounts so were not uniquely identified by GC-FID. Whereas, the major products were oct-1-ene and oct-2-ene with traces of octan-2-one. Similarly, with cyclohexanol the major product was cyclohexene with small amounts of cyclohexanone and dicyclohexylether.

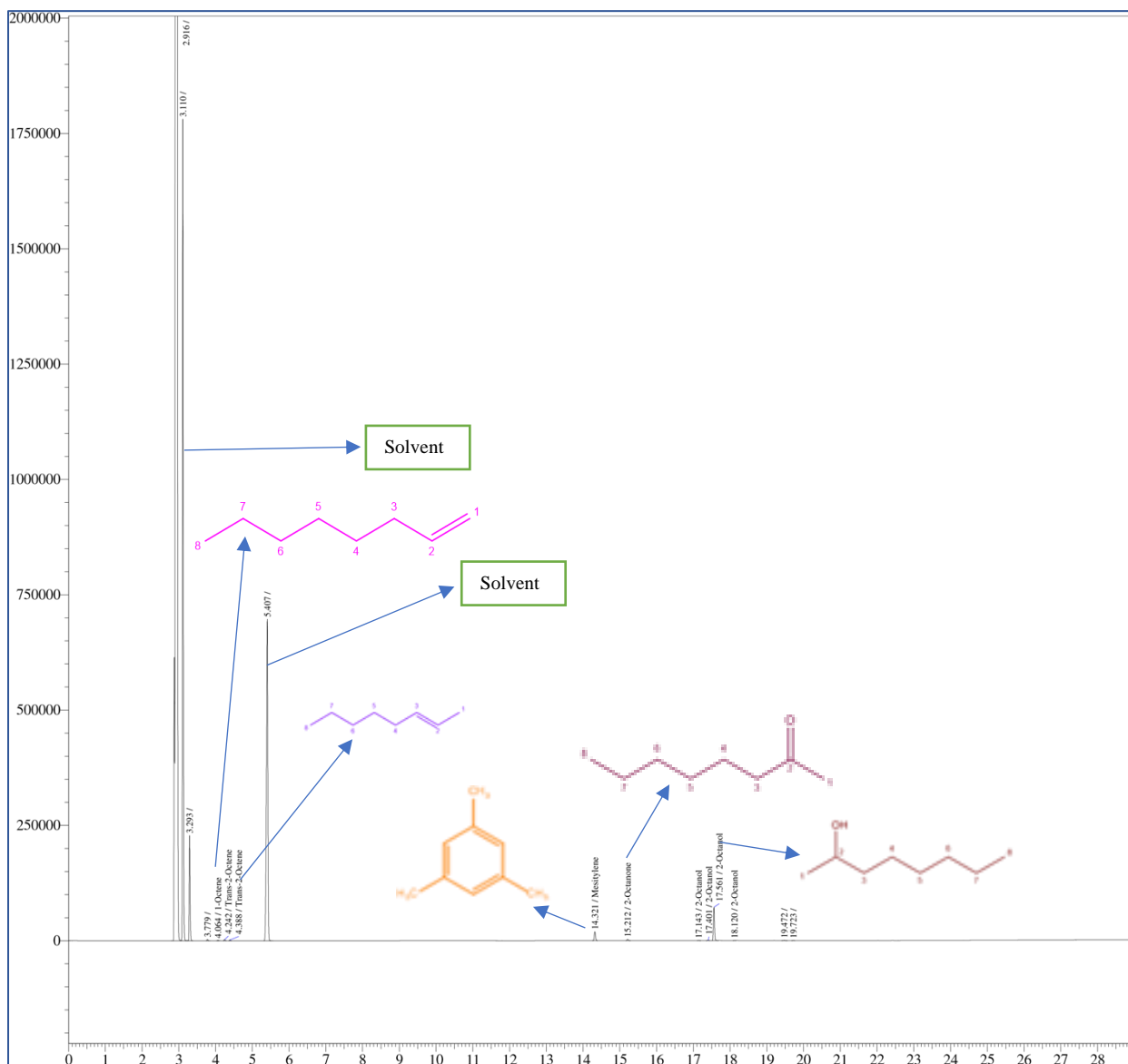


Figure 23. Products of octan-2-ol separation on GC-FID.

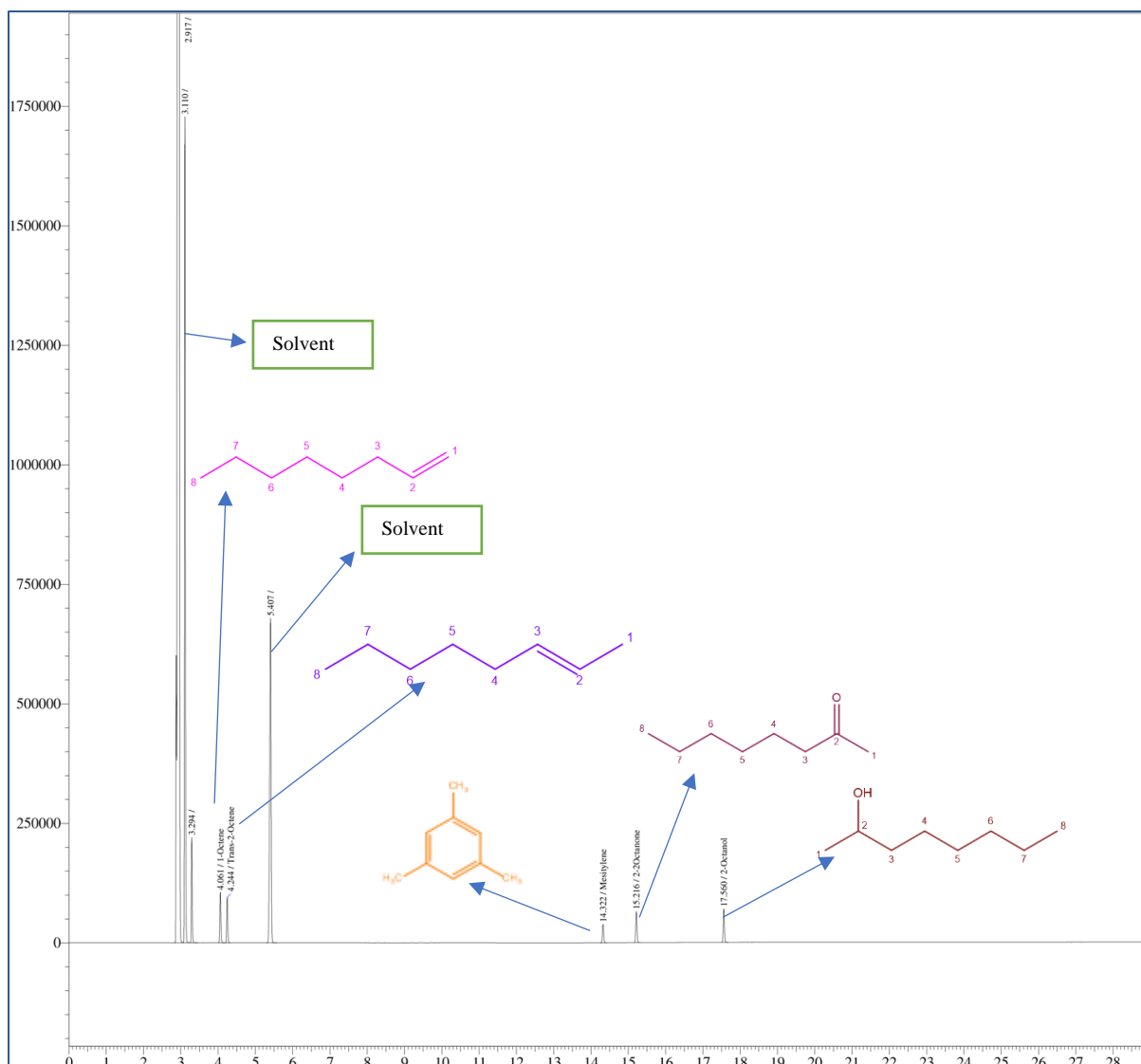


Figure 24. Octan-2-ol standards separation on GC-FID

3.4.3.1 Octan-2-ol Calibration

To quantify reactions involving octan-2-ol in ILs the calibration of octan-2-ol standards was performed. The mass ratios were same as in **Table 7**, although instead of cyclohexanol standards here octan-2-ol, oct-1-ene, trans-2-octene and octan-2-one were calibrated with respect to mesitylene which was again used as the internal standard. The calibration curves obtained are depicted in **Figures 25-28**.

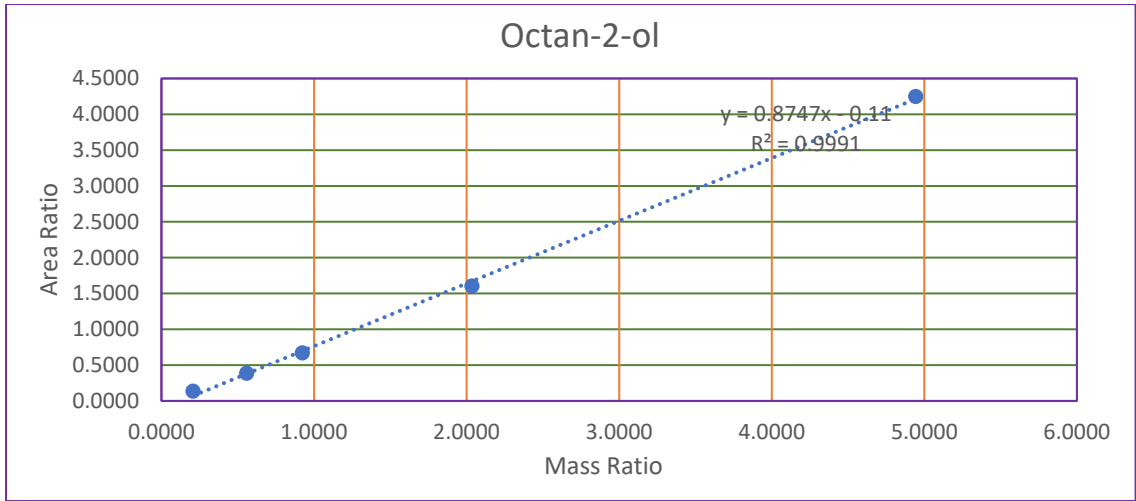


Figure 25. GC-FID Calibration curve of octan-2-ol

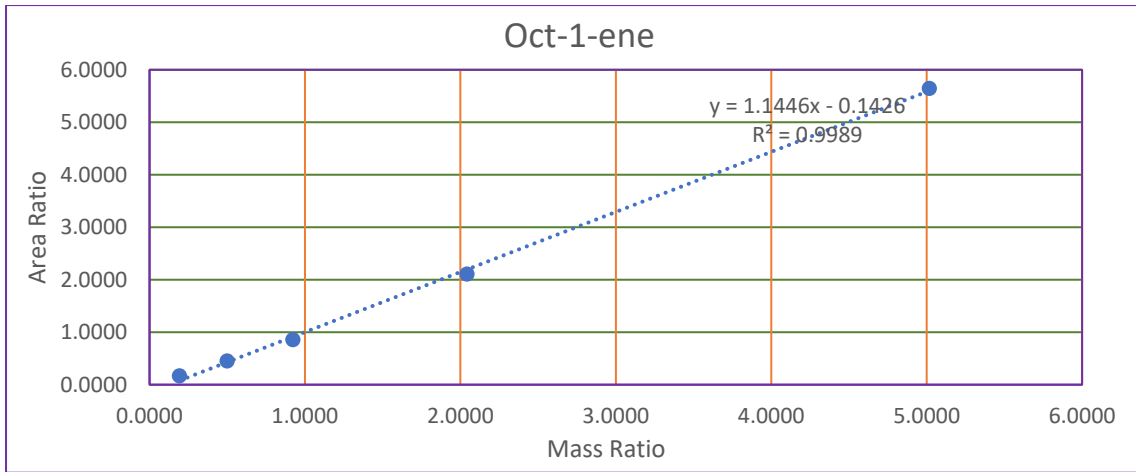


Figure 26. GC-FID Calibration curve of oct-1-ene

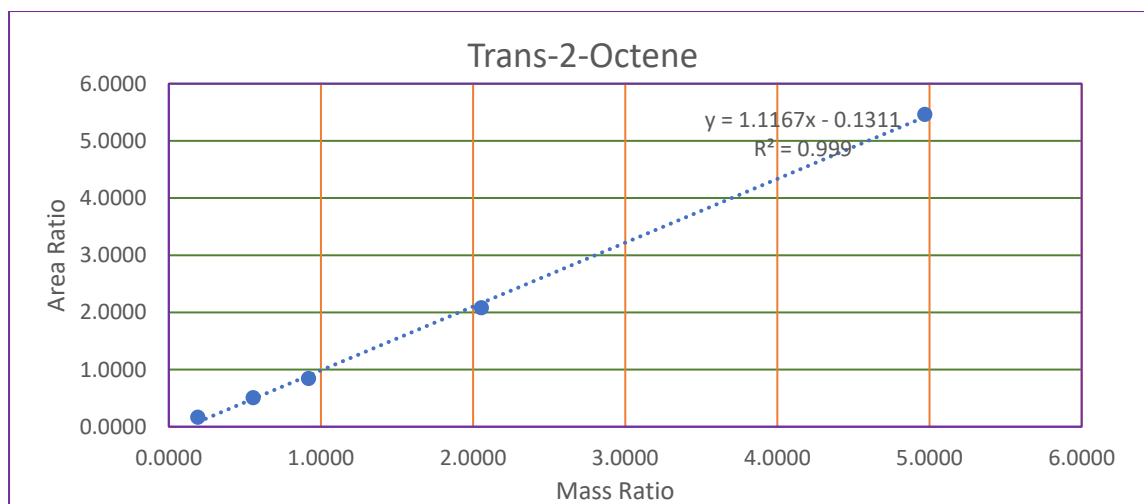


Figure 27. GC-FID Calibration curve of trans-2-octene

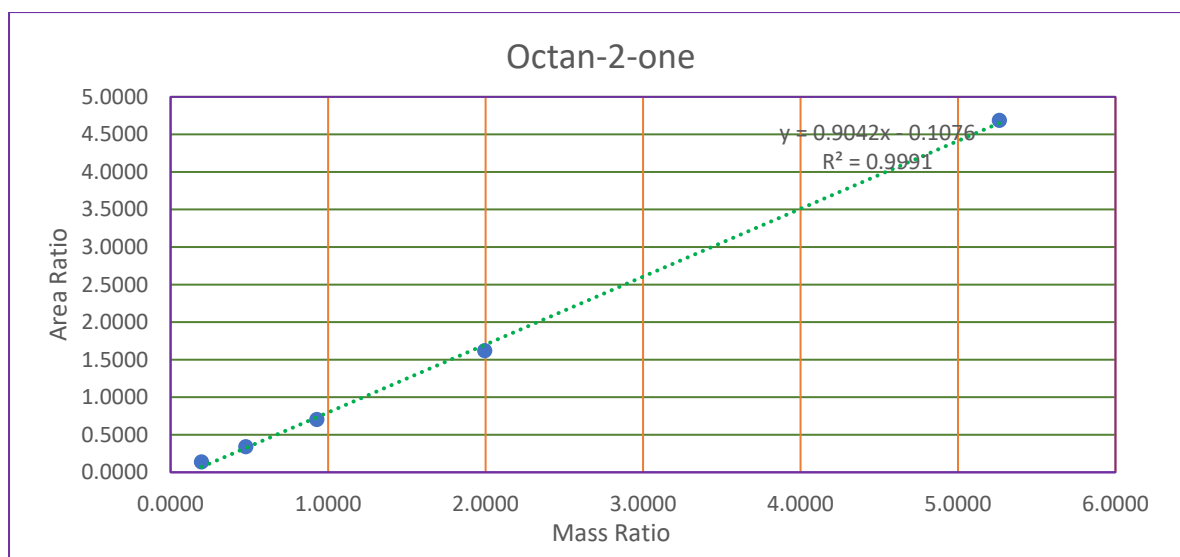


Figure 28. GC-FID Calibration curve of octan-2-one

3.5. Development of an extraction method for the quantification of products

As ILs are non-volatile and cannot be injected into the GC it was necessary to develop an extraction method to quantitatively isolate reactants, products and internal standard from the IL for analysis. To determine the best separation method for IL from products, **Reaction 9 from Table 8** was used to explore different methods of extraction.

3.5.1. Silica Chromatography Column Extraction

The first approach was to explore the removal of the IL on a silica chromatography column while allowing reactants, internal standard and products to pass through. Dichloromethane (0.75mL) was added to the reaction mixture to dissolve all the reactants and products. These were passed through a pipette silica column loading different quantities of the reaction mixture. Each solvent load in the column was collected in a different vial to evaluate where IL breakthrough occurred and whether all reactants and products had been isolated by this stage. Silica column was used to separate the reactants and products as it allows the separation on the basis of polarity of the compounds. As the IL is the most polar component it is expected to elute last, allowing the quantitative recovery of reactants and products.

Using approximately 30 drops of this mixture, it was observed that IL was present in each vial as determined by ¹HNMR. This was due to the high loading of IL in the sample in extraction 1 shown in **Table 8**. The procedure was repeated with one-third as much of the reaction mixture in **extraction 2**. The absence of IL in all vials was observed from ¹HNMR highlighting that it could be successfully removed. Further, we again repeated the process for a different reaction mixture and the results were same, showing that IL was retained on the column under these conditions.

Table 8. Silica column separation of reactions 6 and 8 using dichloromethane as an eluent

Extraction	Reaction	Sample loading and number of extractions
1	9	30 drops of reaction mixture loaded
2	9	10 drops of reaction mixture loaded
3	8	10 drops of reaction mixture loaded

3.6. Extraction methods with quantification of products on GC-FID

While the method described above successfully removed the IL from the solution, allowing it to be analysed by GC, initial experiments made it clear that this approach may not lead to the recovery of all reactants and products as shown in **reaction 9 and 12, Table 9**. To explore the effectiveness of reactant and product quantification we repeated **reaction 9, Table 9** two further times to compare outcomes with the results listed as **reaction 11, Table 9**. These

experiments led to less product formation was observed in comparison to **reaction 9, Table 9** despite using the same reaction conditions and reactant concentrations. We also measured the recovery of cyclohexanol from the initial reaction mixture before reaction and discovered that cyclohexanol was absent which is likely due to retention of cyclohexanol on the column. A small amount of cyclohexanone was also detected by GC-FID in **reaction 12, Table 9**. Modification of the method used to run the column to ensure more solvent remained after each column load improved reproducibility slightly but still only 50% cyclohexanol recovery could be obtained by GC-FID. These results lead to the conclusion that column separation does not allow efficient extraction and quantification of reactants and products.

Table 9. Dehydration of cyclohexanol in [C₁₀C_{1im}][NTf₂] using mesitylene as an internal standard with the quantification of products by GC-FID after separation using a silica. Reported errors are standard deviations of replicate experiments where replicates were performed.

Rxn. No.	Reactants	Mole Fraction Alcohol	Reaction Conditions	Cyclohexanol conversion (%)	Yield Cyclohexene (%)
9.	Cyclohexanol	0.451	150°C	99	31
10.	Cyclohexanol	0.476	120°C	55	0
11.	Cyclohexanol	0.504	150°C	0	14 ± 2
12.*	Cyclohexanol	0.507	No reaction	0	0
13.	Cyclohexanol	0.514	150°C	83	0

★ Time period is 2 hours in each reaction. * Presence of cyclohexanone was identified.

To address the poor recovery using silica column separation, the extraction of the reactants and products with hexane was attempted. Firstly, the final reaction mixture of **reaction 10 and 12, Table 9** was extracted using hexane as it is immiscible with the ionic IL layer. The 0.5mL of reaction mixture 11 was extracted using approx. 2 mL of hexane (5 times) as this reaction mixture remained homogeneous after the reaction was complete. The hexane and IL layers were separated, with the hexane layer analysed by GC-FID to quantify reactants and products. The presence of any residual reactants and products were checked in the IL layer by ¹H NMR.

For **reaction 11** the reaction mixture was heterogeneous and contained oil phase droplets after reaction. Hence the entire remaining reaction mixture was extracted with hexane 5 mL of hexane 10times to ensure complete extraction. ¹H NMR of these reactions indicated that this extraction process was successful in removing the reactants and products.

In **reaction 11, Table 9** with column extraction there was no cyclohexanol detected but, only 14% of cyclohexene was formed as a product. When extracted with hexane as **reaction 15, Table 10** almost complete separation of cyclohexanol was observed. The results from extraction of **reaction 13 and 15** showed good extraction of reactants and products. So, the dehydration reaction of cyclohexanol in [C₁₀C_{1im}][NTf₂] was repeated under similar conditions as shown in **reaction 14, Table 10**. In **reaction 14** the hexane emulsified with the reaction mixture so centrifugation was performed to separate the layers and allow the hexane phase to be removed. The results were different from previous results of **reaction 10** as there was no cyclohexanol with almost 14% of cyclohexene obtained. Further, the reaction was repeated following **procedure 2.3.1** as shown in **reaction 15, 16 Table 10**. The results were consistent with **reaction 13** with only small concentrations of cyclohexene being formed which indicated that the cyclohexene may be retained on the column during the separation.

Table 10. Dehydration of cyclohexanol in [C₁₀C_{1im}][NTf₂] using mesitylene as an internal standard with the quantification of products by GC-FID after hexane extraction. Reported errors are standard deviations of replicate experiments.

Rxn. No.	Mole Fraction Alcohol	Reaction Conditions	Cyclohexanol Conversion (%)	Cyclohexanol Recovered (%)	Yield Cyclohexene (%)
14	0.510	150°C, 2 hours	After Reaction:20	Before reaction: 90	0
15	2 hour: 0.506	150°C, 2 hours	After reaction:12	Before reaction: 84	1.6

Rxn. No.	Mole Fraction Alcohol	Reaction Conditions	Cyclohexanol Conversion (%)	Cyclohexanol Recovered (%)	Yield Cyclohexene (%)
16	4 hour: 0.513	150°C, 4 hours	After reaction: 8	Before reaction: 91	2.1

Given that an apparently more reliable method of extraction had been developed we explored the cyclohexanol reaction in $[C_{10}C_{1im}][NTf_2]$ with slightly increased reaction temperature to obtain higher yields of the desirable products as shown in **reaction 17, 18 and 19 Table 11.** **reaction 19** was performed in duplicate to ensure the consistency of the results obtained. The recovery of cyclohexanol from the original reaction mixture was examined in each case and was found to exceed 99% in all cases.

Table 11. Cyclohexanol dehydration reaction with $[C_{10}C_{1im}][NTf_2]$ and IS at changed reaction conditions.

Rxn. No.	Mole Fraction Alcohol	Reaction Conditions	Cyclohexanol Conversion (%)	Yield Cyclohexene (%)	Yield Cyclohexanone (%)
17	1hour: 0.5117	180°C, 1hour	30	12.5	1.7
18	2hour: 0.5096	180°C, 2 hours	38	21	1.7
19	Vial 1: 0.509	180°C, 3hours	Vial 1 : 43.15	24.80	2
	Vial 2: 0.515	180°C, 3hours	Vial 2: 37	22	3

From **reaction 17, 18 and 19 Table 11** it was evident that cyclohexanol was found to be more reactive at 180°C than 150°C. The separation of reactants and products proceeded to a greater

extent than for the silica column approaches with mass balances > 80% and cyclohexene as the major product after the reaction. While heating this reaction for more prolonged times would likely result in improved yields, the key to our investigation was being able to compare between ILs so the conditions described for **reaction 19** were used as the standard reaction conditions. With average conversions of 40-50% and cyclohexene yields of 25% this provided scope to observe both faster and slower reactions without hitting the limit of detection.

3.7. Cyclohexanol Reactivity with Different Ionic Liquids

As the reliable set of conditions and method for monitoring these reactions was established, the first aim was to explore the effect of alkyl chain attached to the cations in ILs on the reactivity of the reaction.

Table 12. Cyclohexanol reactivity with different [C_nC₁im][NTf₂] ILs at 180°C for 3 hours analysed by GC-FID. Reported errors are standard deviations of replicate experiments.

Rxn. No.	Ionic Liquid	Mole Fraction Alcohol	Cyclohexanol Conversion (%)	Yield Cyclohexene (%)	Yield Cyclohexanone (%)
20	[C ₁₀ C ₁ im][NTf ₂]	0.512	43 ± 8	25 ± 4	2.50 ± 0.74
21	[C ₈ C ₁ im][NTf ₂]	0.546	38.4 ± 1.9	26.03 ± 0.01	1.76 ± 0.02
22	[C ₆ C ₁ im][NTf ₂]	0.469	51.5 ± 1.1	37.32 ± 0.10	1.67 ± 0.12

Rxn. No.	Ionic Liquid	Mole Fraction Alcohol	Cyclohexanol Conversion (%)	Yield Cyclohexene (%)	Yield Cyclohexanone (%)
23	[C ₄ C ₁ im] [NTf ₂]	0.476	57.9 ± 0.6	38.74 ± 0.02	1.9 ± 0.1
24	[C ₂ C ₁ im] [NTf ₂]	0.454	59 ± 5	38.70 ± 0.1	2.1 ± 0.1

The results from **reaction 20, 21, 22, 23 and 24, Table 12** confirm that with the decrease in alkyl chain length the formation of products increases. The decrease in alkyl chain length of the IL reduces the relative volume of the non-polar domains of the IL. This will lead to cyclohexanol being solvated to a greater extent in the polar region and would account for the more effective reaction in [C₂C₁im] [NTf₂] as compared to [C₁₀C₁im] [NTf₂]. This will be discussed in more detail in light of the proposed mechanism in the following sections.

3.8. Effect of Cyclohexanol Mole Fraction on Reactivity

In order to see the effect of the mole fraction of cyclohexanol on the effectiveness of the dehydration reaction and whether the concentration of IL affects to the reaction, the cyclohexanol reaction was monitored at different concentrations in [C₁₀C₁im][NTf₂] and even without the IL present. The mole fraction of alcohol without the IL present was 0.9 rather than 1 due to the presence of the mesitylene internal standard.

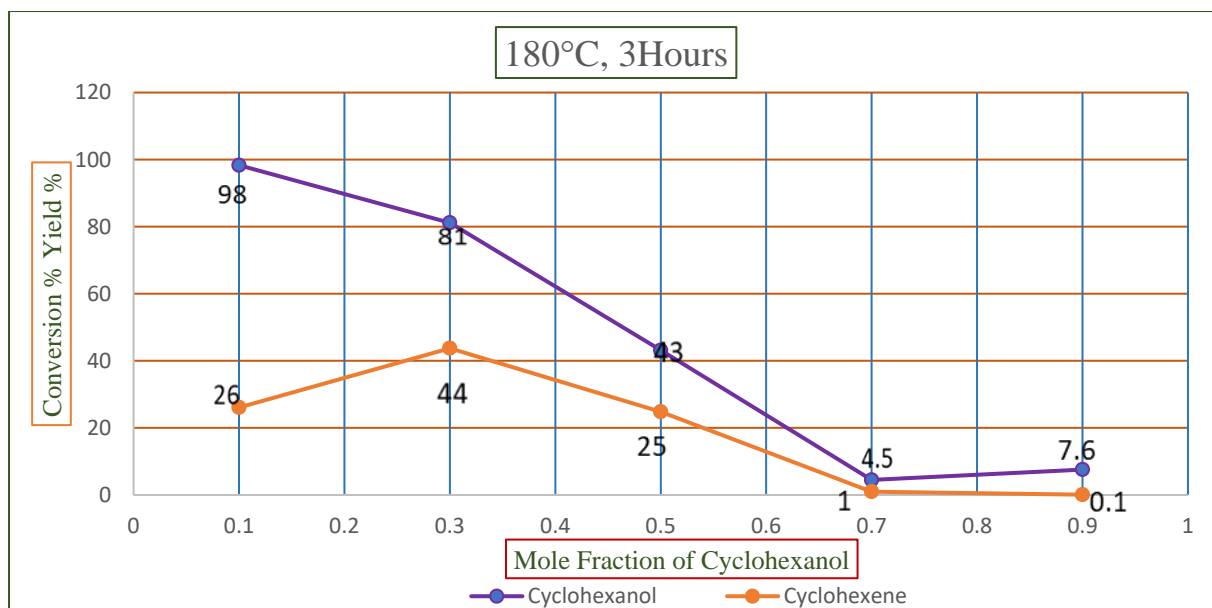


Figure 29. Cyclohexanol conversion and cyclohexene yield at different mole fraction of cyclohexanol in $[C_{10}C_{11}m]$ $[NTf_2]$.

The results from **Figure 29** shown the effect of the alcohol mole fraction on reactivity. It is evident from **Figure 29** that with the increase in mole fraction of cyclohexanol the yield of cyclohexene increases to a maximum at 0.3 mole fraction and then decreases. Apparent conversion decreases consistently with increased alcohol mole fraction but at low mole fractions it is possible that this may be affected by the incomplete extraction of cyclohexanol. The highest mole fraction consisting of with approx. 1mL of cyclohexanol without IL in the reaction mixture does not show any significant reaction in terms of the yield of cyclohexene. This indicates that IL is not only acting as a solvent but, also acting as a catalyst for the reaction.

In order to rule out the possibility of Lewis acid catalysis arising from lithium ions present as impurities from the IL synthesis, the ILs used in **Table 11** were analyzed using ICP-MS. Lithium concentrations in these ILs were all below the level of detection indicating that the reaction is facilitated by the IL itself not a Lewis acidic synthesis impurity.

After seen the affect the alkyl chains and different mole fraction of alcohol on the reactivity the next step was to explore the effect of different anions attached to the ILs towards the dehydration reaction.

3.9. Effect of Ionic Liquid Anion on Cyclohexanol Dehydration

To assess the effect of the IL anion on the dehydration of cyclohexanol, its reaction in [C₁₀C_{1im}][OTf], [C₄C_{1im}][OTf], [C₄C_{1im}][Me₂PO₄] and [C₄C_{1im}][N(CN)₂] was explored. These results are summarized in **Table 13**.

Table 13. Quantification of products on GC-FID after cyclohexanol reactivity with two [OTf] (reaction 25, 26), [C₁₀C_{1im}][Me₂PO₄] and, [C₄C_{1im}][N(CN)₂] (reaction 29, 30) ILs at 180°C for 3 hours and with same temperature and same [OTf] ILs for 18 hours (reaction 27, 28)

Rxn. No.	Ionic Liquid	Mole Fraction Alcohol	Cyclohexanol Conversion (%)	Yield Cyclohexene (%)	Yield Cyclohexanone (%)
25	[C ₁₀ C _{1im}][OTf]	0.405	14 ± 2	5 ± 2	2 ± 0.3
26	[C ₄ C _{1im}][OTf]	0.311	0*	0.55 ± 0.06	2.43 ± 0.02
27	[C ₁₀ C _{1im}][OTf]	0.425	10 ± 3	13 ± 1.8	2.7 ± 0.3
28	[C ₄ C _{1im}][OTf]	0.329	0*	2.23 ± 0.27	2.42 ± 0.04
29	[C ₁₀ C _{1im}][Me ₂ PO ₄]	0.423	42 ± 6	0.32 ± 0.09	1.3 ± 0.3
30	[C ₄ C _{1im}][N(CN) ₂]	0.298	0*	0.65 ± 0.05	1.83 ± 0.05
31	No IL	0.855	8 ± 0.01	0.08 ± 0.01	1 ± 0.02

**Cyclohexanol recovery was over 100% based on GC-FID result.*

The number of extractions steps undertaken with these ILs was increased for better separation due to the increased hydrophilicity of these anions. **Reaction 25 and 26, Table 13** indicates that cyclohexanol does not react as readily in [C_nC_{1im}][OTf]. ILs as compared to their [NTf₂] equivalents. As the [OTf]⁻ is more basic than [NTf₂]⁻ this indicates that as the anion basicity increases, the rate of the dehydration reaction decreases. This trend was also evident for the

other ILs with low yields of cyclohexene also observed within $[\text{C}_4\text{C}_{1\text{im}}][\text{Me}_2\text{PO}_4]$ and $[\text{C}_4\text{C}_{1\text{im}}][\text{N}(\text{CN})_2]$ **reaction 29 and 30, Table 13.**

Despite the low yield of cyclohexene, the conversion of cyclohexanol was relatively high in $[\text{C}_{10}\text{C}_{1\text{im}}][\text{Me}_2\text{PO}_4]$. The presence of a side reaction was evident from ^{31}P NMR of the **reaction mixture 29** shown from **Figure 30**. The peak at -1.49 ppm not present in the original IL is evidence of side reaction between cyclohexanol and the $[\text{Me}_2\text{PO}_4]^-$ anion. This is most likely due to the phosphorylation of alcohols.

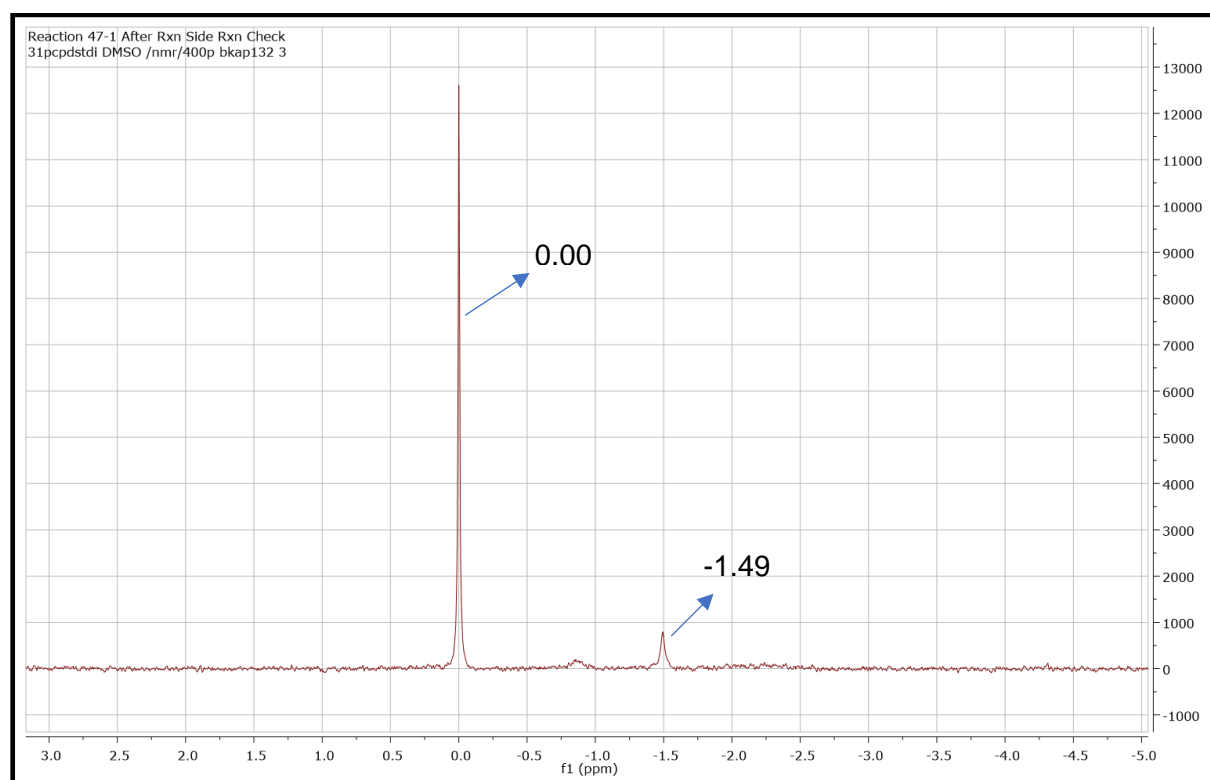


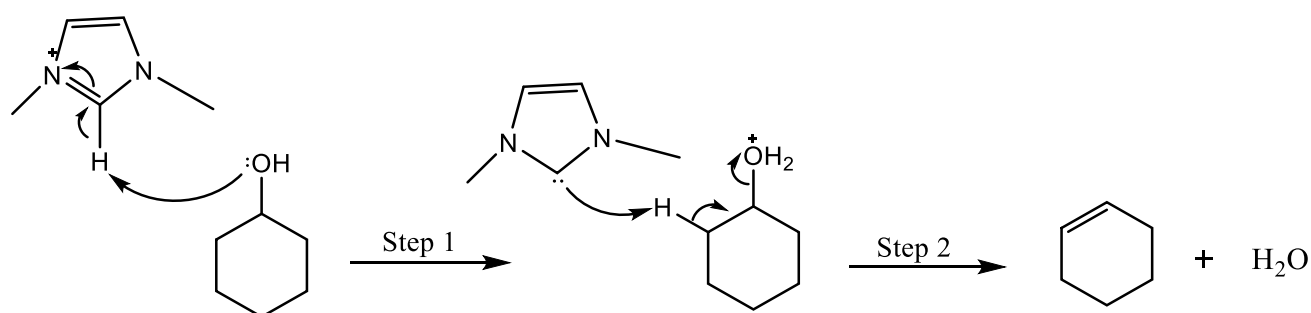
Figure 30. ^{31}P NMR of reaction 23 after reaction.

Moreover, with the increase in alkyl chain for the $[\text{OTf}]^-$ ILs the reactivity decreases, the exact opposite trend to that observed for the $[\text{NTf}_2]^-$ ILs. In an attempt to achieve higher reaction yields for comparison, the reaction time was raised to 18 hours but the product yield and conversion did not increase significantly compared to the 3 hour reactions seen for **reaction 25 and 26.**

3.10. Mechanism of Cyclohexanol Dehydration in Ionic Liquids

The ILs worked as an effective catalyst for the dehydration of cyclohexanol as shown from the above results. A possible mechanism that would be consistent with the greater reactivity of

cyclohexanol within the $[\text{NTf}_2]^-$ ILs in comparison to the $[\text{OTf}]^-$ and $[\text{N}(\text{CN})_2]^-$ ILs is shown in **Scheme 19**. Generally the rate of an elimination reaction depends on the concentration of reactants. Whereas, here it was revealed that increasing the mole fraction of reactants in the mixture led to product formation, and hence the rate of reaction, decreasing above a mole fraction of 0.3. This demonstrated that the IL was essential in the rate determining step of the dehydration reaction.



Scheme 19. Proposed mechanism for the dehydration of cyclohexanol in ILs.

The proposed mechanism in **Scheme 19** is consistent with the observations of the reactivity of cyclohexanol in ILs. In the case of $[\text{NTf}_2]^-$ ILs, the anion more weakly interacts with the most acidic hydrogen in the imidazolium cation, which makes the proton more easily available for the protonation of the alcohol as shown in step 1. The next steps can either proceed via an E_1 mechanism with the loss of water followed by the attack of the base or an E_2 mechanism where the base attacks simultaneously, leading to the formation of the desired alkene product. Whereas, in case of $[\text{OTf}]^-$ the cation and anion more strongly interact so the hydrogen is not easily available for protonation of the alcohol leading to its reduced reactivity.

The $[\text{NTf}_2]^-$ ILs with longer alkyl chains were found to reduce reactivity whereas the $[\text{OTf}]^-$ ILs with longer alkyl chains were found to lead to increased reactivity. The explanation for this lies in considering the effect of the amphiphilic nanostructure. As the $[\text{NTf}_2]^-$ anion is more hydrophobic than the $[\text{OTf}]^-$ anion it will lead to greater partitioning of the cyclohexanol outside of the polar region of the IL. These non-polar regions are not catalytically active as they do not contain the imidazolium cation, as implicated in the mechanism shown in **Scheme 19**. Hence for the $[\text{C}_n\text{C}_{1}\text{im}][\text{NTf}_2]$ series the longer alkyl chain leads to reduced concentrations of cyclohexanol dissolved in the catalytically active regions. For the more basic $[\text{OTf}]^-$ anion the cyclohexanol will preferentially partition in the polar region. As the non-polar region increases in size the effective concentration of cyclohexanol increases leading to an increased

rate of reaction, as has been observed for polar reactants in nucleophilic substitution reactions.⁵³⁻⁵⁴

3.11. Reactivity of Octan-2-ol within Ionic Liquids

The new reactions of octan-2-ol were run as shown in **reaction 32, 33, 34 and, 35 Table 14** to demonstrate the effects of ILs under set the reaction conditions as in **reaction 19, Table 11**. Octan-2-ol standards were calibrated on GC-FID as shown in **section 3.4.3.1**.

Table 14. Quantification of products on GC-FID after octan-2-ol reactivity with ILs containing [NTf₂]⁻ and [OTf]⁻ anion with different alkyl chains at 180°C for 3 hours.

Rxn. No.	Ionic Liquid	Mole Fraction Alcohol	Octan-2-ol Conversion (%)	Yield Oct-1-ene (%)	Yield Trans-2-octene (%)	Yield Octan-2-one (%)
32	[C ₁₀ C ₁ im] [NTf ₂]	0.399	9 ± 4	0.7 ± 0.3	1.9 ± 0.8	3.97 ± 0.03
33	[C ₄ C ₁ im] [NTf ₂]	0.357	62 ± 8	6.7 ± 1	15 ± 2	3.63 ± 0.16
34	[C ₁₀ C ₁ im] [OTf]	0.372	0*	0.59 ± 0.07	2 ± 0.4	3.8 ± 0.3
35	[C ₄ C ₁ im] [OTf]	0.299	0*	0.17 ± 0.08	0.29 ± 0.08	4.4 ± 0.2

**Octan-2-ol recovery was over 100% based on GC-FID result.*

In the case of the reaction with [C₁₀C₁im][NTf₂] 9% conversion was achieved which is lower than cyclohexanol under the comparable conditions. From this it was seen that NTf₂ is less reactive towards octan-2-ol. Whereas, [C₁₀C₁im][OTf] and [C₄C₁im][OTf] didn't lead to any significant reaction of octan-2-ol as nearly complete recovery could be observed by GC-FID. The alkyl chain effect was the same, if not even more pronounced, than for cyclohexanol with the dehydration in [C₁₀C₁im][NTf₂] proceeding substantially less reactive than [C₄C₁im][NTf₂] with the opposite trend observed for the [OTf]⁻ ILs. Due to the less stability of carbocation

during the reaction with NTf_2 and triflates shown less reactivity towards dehydration of octan-2-ol. It is suggested that the proposed mechanism and solvent effects might be able to be generalized to other alcohols.

CHAPTER 4: CONCLUSIONS & FUTURE WORK

4.1. Conclusions

Imidazolium ILs were utilized as solvents and their effects on substitution reactions where the ILs acts as catalyst was studied. The scope of the project was to perform with imidazolium ILs as these have been widely studied and their solution structures are well known. By using the ILs as catalyst the use of acids can be reduced that are harmful for the environment.

The dehydration reactions of the secondary alcohols cyclohexanol and octan-2-ol within ILs demonstrated the effects of ILs on the reactivity of these alcohols. The dehydration of alcohols to alkenes did not readily occur at temperatures of $<150^{\circ}\text{C}$. Whereas, after a series of reactions at different temperatures the dehydration of cyclohexanol and octan-2-ol could be observed after 3 hours at 180°C .

Generally the rate of an elimination reaction depends on the concentration of reactants. Whereas, here it was revealed that increasing the mole fraction of reactants in the mixture led to product formation, and hence the rate of reaction, decreasing above a mole fraction of 0.3. This demonstrated that the IL was essential in the rate determining step of the dehydration reaction. In ILs there are intermolecular interactions that results in amphiphilic nanostructure with specified cationic and anionic regions. Specifically it was suggested that the imidazolium cation protonates the alcohol, forming a carbene intermediate which completes the elimination reaction to regenerate the imidazolium cation. This mechanism suggests that the reaction should proceed in the polar regions of the IL where the ions are in close proximity to the alcohol.

Furthermore, the alkyl chain attached to the cation affects the reactivity of alcohols explored in this project. As the alkyl chain increases the product formation also increases in case of ILs containing the hydrophilic anion $[\text{OTf}]^{-}$ whereas it was reverse for ILs containing the hydrophobic anion $[\text{NTf}_2]^{-}$. With the long alkyl chains attached to the cation, the alcohol molecules remain in the nonpolar region for longer timeframes when a hydrophobic anion is present. These regions are not catalytically active and so a slower reaction results. The opposite is true when a more hydrophilic anion is present due to the increased relative concentration of alcohol in the polar regions which proportionally increases as the alkyl chain length increases.

4.2. Future Work

To test the mechanism proposed for the imidazolium ILs, a future goal would be to examine the effect of reducing the availability of the C²-H proton. The easiest way to design this is to use an IL containing a methyl group attached to the C² position of the imidazolium ring. The acidity of C² have been reported to be tested in reaction of CO₂ in [C₂C₁im][OAc].⁵⁵ The reactivity of alcohols within this IL will inform whether the acidity of the C²-H proton is critical to the observed activity. The deuteration of proton can also be applied to see the effect. The deuterium would end up on the product if the breaking of the C-D bond happens during the reaction. If it doesn't then the deuterium would remain on the IL. Alternatively, to make the protonation inoperative another cation such as N-alkyl-pyridinium, tetraalkyl-ammonium and tetraalkyl-phosphonium can be used for this reaction.

As the imidazolium ILs were found to be effective with the secondary alcohols. The effect of imidazolium cations on primary alcohols and tertiary alcohols at high temperature can be further explored by changing the anions in ILs.

References

1. P, W., P. Walden, Ueber die Molekulargröße und elektrische Leitfähigkeit einiger geschmolzenen Salze, . *Bulletin de l'Académie Impériale des Sciences de St.-Petersbourg. VI série* **1914**, 8 (6), 405-422.
2. Hurley, F. H.; Wier, T. P., Electrodeposition of Metals from Fused Quaternary Ammonium Salts. *Journal of The Electrochemical Society* **1951**, 98 (5), 203.
3. Wilkes, J. S.; Zaworotko, M. J., Air and water stable 1-ethyl-3-methylimidazolium based ionic liquids. *Journal of the Chemical Society, Chemical Communications* **1992**, (13), 965-967.
4. Bonhôte, P.; Dias, A.-P.; Papageorgiou, N.; Kalyanasundaram, K.; Grätzel, M., Hydrophobic, Highly Conductive Ambient-Temperature Molten Salts. *Inorganic Chemistry* **1996**, 35 (5), 1168-1178.
5. El-Harbawi, M., Toxicity Measurement of Imidazolium Ionic Liquids Using Acute Toxicity Test. *Procedia Chemistry* **2014**, 9, 40-52.
6. Welton, T. J. B. R., Ionic liquids: a brief history. **2018**, 10 (3), 691-706.
7. Amde, M.; Liu, J.-F.; Pang, L., Environmental Application, Fate, Effects, and Concerns of Ionic Liquids: A Review. *Environmental Science & Technology* **2015**, 49 (21), 12611-12627.
8. Petkovic, M.; Ferguson, J.; Bohn, A.; Trindade, J.; Martins, I.; Carvalho, M.; Leitão, M.; Rodrigues, C.; Garcia, H.; Ferreira, R.; Seddon, K.; Rebelo, L. P. N.; Silva Pereira, C., Exploring fungal activity in the presence of ionic liquids. *Green Chemistry* **2009**, 11, 889-894.
9. Peric, B.; Sierra, J.; Martí, E.; Cruañas, R.; Garau, M. A., A comparative study of the terrestrial ecotoxicity of selected protic and aprotic ionic liquids. *Chemosphere* **2014**, 108, 418-425.
10. Bernot, R. J.; Brueseke, M. A.; Evans-White, M. A.; Lamberti, G. A., Acute and chronic toxicity of imidazolium-based ionic liquids on *Daphnia magna*. *Environmental Toxicology and Chemistry* **2005**, 24 (1), 87-92.
11. Romero, A.; Santos, A.; Tojo, J.; Rodríguez, A., Toxicity and biodegradability of imidazolium ionic liquids. *Journal of Hazardous Materials* **2008**, 151 (1), 268-273.
12. Petkovic, M.; Seddon, K. R.; Rebelo, L. P. N.; Silva Pereira, C., Ionic liquids: a pathway to environmental acceptability. *Chemical Society Reviews* **2011**, 40 (3), 1383-1403.
13. Hayes, R.; Warr, G. G.; Atkin, R., Structure and Nanostructure in Ionic Liquids. *Chemical Reviews* **2015**, 115 (13), 6357-6426.
14. Ghandi, K., A Review of Ionic Liquids, Their Limits and Applications. *Green and Sustainable Chemistry* **2013**, 04.
15. Miran, M. S.; Kinoshita, H.; Yasuda, T.; Susan, M. A. B. H.; Watanabe, M., Hydrogen bonds in protic ionic liquids and their correlation with physicochemical properties. *Chemical Communications* **2011**, 47 (47), 12676-12678.
16. Tsuzuki, S.; Shinoda, W.; Miran, M. S.; Kinoshita, H.; Yasuda, T.; Watanabe, M., Interactions in ion pairs of protic ionic liquids: Comparison with aprotic ionic liquids. *The Journal of Chemical Physics* **2013**, 139 (17), 174504.
17. Vashchuk, A.; Fainleib, A.; Starostenko, O.; Grande, D., Application of ionic liquids in thermosetting polymers: Epoxy and cyanate ester resins. *Express Polymer Letters* **2018**, 12, 898-917.
18. Lui, M. Y.; Crowhurst, L.; Hallett, J. P.; Hunt, P. A.; Niedermeyer, H.; Welton, T., Salts dissolved in salts: ionic liquid mixtures. *Chemical Science* **2011**, 2 (8), 1491-1496.

19. Matthews, R. P.; Villar-Garcia, I. J.; Weber, C. C.; Griffith, J.; Cameron, F.; Hallett, J. P.; Hunt, P. A.; Welton, T., A structural investigation of ionic liquid mixtures. *Physical Chemistry Chemical Physics* **2016**, *18* (12), 8608-8624.
20. Skarmoutsos, I.; Welton, T.; Hunt, P. A., The importance of timescale for hydrogen bonding in imidazolium chloride ionic liquids. *Physical Chemistry Chemical Physics* **2014**, *16* (8), 3675-3685.
21. Wang, Y.-L.; Laaksonen, A.; Fayer, M. D., Hydrogen Bonding versus π - π Stacking Interactions in Imidazolium–Oxalatoaluminate Ionic Liquid. *The Journal of Physical Chemistry B* **2017**, *121* (29), 7173-7179.
22. Dong, K.; Zhang, S., Hydrogen Bonds: A Structural Insight into Ionic Liquids. **2012**, *18* (10), 2748-2761.
23. Avent, A. G.; Chaloner, P. A.; Day, M. P.; Seddon, K. R.; Welton, T., Evidence for hydrogen bonding in solutions of 1-ethyl-3-methylimidazolium halides, and its implications for room-temperature halogenoaluminate(III) ionic liquids. *Journal of the Chemical Society, Dalton Transactions* **1994**, (23), 3405-3413.
24. Fumino, K.; Wulf, A.; Ludwig, R., The Cation–Anion Interaction in Ionic Liquids Probed by Far-Infrared Spectroscopy. *Angewandte Chemie International Edition* **2008**, *47* (20), 3830-3834.
25. Dong, K.; Zhang, S.; Wang, J., Understanding the hydrogen bonds in ionic liquids and their roles in properties and reactions. *Chemical Communications* **2016**, *52* (41), 6744-6764.
26. Yokozeki, A.; Kasprzak, D. J.; Shiflett, M. B., Thermal effect on C–H stretching vibrations of the imidazolium ring in ionic liquids. *Physical Chemistry Chemical Physics* **2007**, *9* (36), 5018-5026.
27. Hunt, P. A.; Ashworth, C. R.; Matthews, R. P., Hydrogen bonding in ionic liquids. *Chemical Society Reviews* **2015**, *44* (5), 1257-1288.
28. Hunt, P. A.; Gould, I. R., Structural Characterization of the 1-Butyl-3-methylimidazolium Chloride Ion Pair Using ab Initio Methods. *The Journal of Physical Chemistry A* **2006**, *110* (6), 2269-2282.
29. Schröder, U.; Wadhawan, J. D.; Compton, R. G.; Marken, F.; Suarez, P. A. Z.; Consorti, C. S.; de Souza, R. F.; Dupont, J., Water-induced accelerated ion diffusion: voltammetric studies in 1-methyl-3-[2,6-(S)-dimethylocten-2-yl]imidazolium tetrafluoroborate, 1-butyl-3-methylimidazolium tetrafluoroborate and hexafluorophosphate ionic liquids. *New Journal of Chemistry* **2000**, *24* (12), 1009-1015.
30. Wang, Y.; Voth, G. A., Unique Spatial Heterogeneity in Ionic Liquids. *Journal of the American Chemical Society* **2005**, *127* (35), 12192-12193.
31. Triolo, A.; Russina, O.; Bleif, H.-J.; Di Cola, E., Nanoscale Segregation in Room Temperature Ionic Liquids. *The Journal of Physical Chemistry B* **2007**, *111* (18), 4641-4644.
32. Rodenbücher, C.; Wippermann, K.; Korte, C., Atomic Force Spectroscopy on Ionic Liquids. *Applied Sciences* **2019**, *9* (11).
33. Pontoni, D.; DiMichiel, M.; Deutsch, M., Temperature evolution of the bulk nanostructure in a homologous series of room temperature ionic liquids. *Journal of Molecular Liquids* **2020**, *300*, 112280.
34. Russina, O.; Triolo, A.; Gontrani, L.; Caminiti, R., Mesoscopic Structural Heterogeneities in Room-Temperature Ionic Liquids. *The Journal of Physical Chemistry Letters* **2012**, *3* (1), 27-33.
35. McMurry, J., *Organic Chemistry*. 6 ed.; David Harris: United States Of America, 2004; p 1176.
36. *Organic chemistry*. Libre Texts Libraries: 2020.

37. Manabe, K.; Iimura, S.; Sun, X.-M.; Kobayashi, S., Dehydration Reactions in Water. Brønsted Acid–Surfactant-Combined Catalyst for Ester, Ether, Thioether, and Dithioacetal Formation in Water. *Journal of the American Chemical Society* **2002**, *124* (40), 11971-11978.
38. Kalviri, H. A.; Kerton, F. M., Dehydration of Benzyl Alcohols in Phosphonium Ionic Liquids: Synthesis of Ethers and Alkenes. *Advanced Synthesis & Catalysis* **2011**, *353* (17), 3178-3186.
39. Kalviri, H. A.; Petten, C. F.; Kerton, F. M., Catalytic dehydrative etherification and chlorination of benzyl alcohols in ionic liquids. *Chemical Communications* **2009**, (34), 5171-5173.
40. Kumar, R.; Sharma, A.; Sharma, N.; Kumar, V.; Sinha, A., Neutral Ionic Liquid [hmim]Br as a Green Reagent and Solvent for the Mild and Efficient Dehydration of Benzyl Alcohols into (E)-Arylalkenes Under Microwave Irradiation. *European Journal of Organic Chemistry* **2008**, *2008*, 5577-5582.
41. Weber, C. C.; Brooks, N. J.; Castiglione, F.; Mauri, M.; Simonutti, R.; Mele, A.; Welton, T., On the structural origin of free volume in 1-alkyl-3-methylimidazolium ionic liquid mixtures: a SAXS and ¹²⁹Xe NMR study. *Physical Chemistry Chemical Physics* **2019**, *21* (11), 5999-6010.
42. Brooks, N. J.; Castiglione, F.; Doherty, C. M.; Dolan, A.; Hill, A. J.; Hunt, P. A.; Matthews, R. P.; Mauri, M.; Mele, A.; Simonutti, R.; Villar-Garcia, I. J.; Weber, C. C.; Welton, T., Linking the structures, free volumes, and properties of ionic liquid mixtures. *Chemical Science* **2017**, *8* (9), 6359-6374.
43. Yalcin, D.; Welsh, I. D.; Matthewman, E. L.; Jun, S. P.; McKeever-Willis, M.; Gritcan, I.; Greaves, T. L.; Weber, C. C., Structural investigations of molecular solutes within nanostructured ionic liquids. *Physical Chemistry Chemical Physics* **2020**, *22* (20), 11593-11608.
44. Earl, G. W.; Weisshaar, D. E.; Paulson, D.; Hanson, M.; Uilk, J.; Wineinger, D.; Moeckly, S., Quaternary methyl carbonates: Novel agents for fabric conditioning. *Journal of Surfactants and Detergents* **2005**, *8* (4), 325-329.
45. Wang, Y.; Li, H.-R.; Wu, T.; Wang, C.-M.; Han, S.-J., Reaction mechanism study for the synthesis of alkylimidazolium-based Halide Ionic liquids. *21* **2005**, *5*, 517-522.
46. Kuhlmann, E.; Himmler, S.; Giebelhaus, H.; Wasserscheid, P., Imidazolium dialkylphosphates—a class of versatile, halogen-free and hydrolytically stable ionic liquids. *Green Chemistry* **2007**, *9* (3), 233-242.
47. Priede, E.; Bakis, E.; Zicmanis, A., When Chlorides are the Most Reactive: A Simple Route towards Diverse Mono-and Dicationic Dimethyl Phosphate Ionic Liquids. *Synlett* **2014**, 25.
48. Ignat'ev, N. V.; Barthen, P.; Kucheryna, A.; Willner, H.; Sartori, P., A Convenient Synthesis of Triflate Anion Ionic Liquids and Their Properties. *Molecules* **2012**, *17* (5).
49. A.A, S.; K.A, D., Synthesizing of ionic liquids from different chemical reactions. *Journal of Scientific Research I* **2011**, *3*, 246-252.
50. Avola, S.; Goettmann, F.; Antonietti, M.; Kunz, W., Organic reactivity of alcohols in superheated aqueous salt solutions: an overview. *New Journal of Chemistry* **2012**, *36* (8), 1568-1573.
51. Whitmore, F. C.; Rowland, C. S.; Wrenn, S. N.; Kilmer, G. W., The Dehydration of Alcohols. XIX.1-4 t-Amyl Alcohol and the Related Dimethylneopentylcarbinol. *Journal of the American Chemical Society* **1942**, *64* (12), 2970-2972.

52. Yang, B.-L.; Maeda, M.; Goto, S., Kinetics of liquid phase synthesis of tert-amyl methyl ether from tert-amyl alcohol and methanol catalyzed by ion exchange resin. *International Journal of Chemical Kinetics* **1998**, *30* (2), 137-143.
53. Weber, C. C.; Masters, A. F.; Maschmeyer, T., Pseudo-Encapsulation—Nanodomains for Enhanced Reactivity in Ionic Liquids. *Angewandte Chemie International Edition* **2012**, *51* (46), 11483-11486.
54. Weber, C. C.; Masters, A. F.; Maschmeyer, T., Steric, hydrogen-bonding and structural heterogeneity effects on the nucleophilic substitution of N-(p-fluorophenyldiphenylmethyl)-4-picolinium chloride in ionic liquids. *Organic & Biomolecular Chemistry* **2013**, *11* (15), 2534-2542.
55. Daud, N. M. A. N.; Bakis, E.; Hallett, J. P.; Weber, C. C.; Welton, T., Evidence for the spontaneous formation of N-heterocyclic carbenes in imidazolium based ionic liquids. *Chemical Communications* **2017**, *53* (81), 11154-11156.